Egypt. J. Chem. **Vol.** 68, SI: Z. M. Nofal, pp. 1111- 1134(2025)

Egyptian Journal of Chemistry

http://ejchem.journals.ekb.eg/

Comparative Study of Biocompatibility and Toxicity of Chemical and Green Synthesized Silver Nanoparticles

Heba Badou Ibrahim[1], Emam Abdel-Mobdy Abdel-Rahim[1], Mohamed Abdel-Shakur Ali[1*]

[1]*Biochemistry department, Faculty of agriculture, Cairo University, Giza, Egypt*

Abstract

Silver nanoparticles (AgNPs) can be utilized in abroad fascinating biomedical, industrial, and agricultural applications, so they are in increasing demand. However, the ability of AgNPs to accumulate in the human body may cause side effects on various organs. Pomegranate peel extract (PPE) showed biological activity as a protective agent against hepatic and renal diseases. The present study aimed to biosynthesize AgNPs using PEE (PPE-AgNPs) compared to starch (ST-AgNPs), PPE/ST-AgNPs, and chemical synthesis nanoparticles $NaBH_4$-AgNPs to study the physicochemical characteristics of NPs, determine the antioxidant activity and evaluate their biochemical toxicity *in vivo*. Different synthesized AgNPs were characterized by Ultraviolet-visible (UV-VIS) spectrophotometer, Fourier transform infrared (FTIR), ZetaSizer, and transmission electron microscope (TEM). Fifty five male albino rats were divided into 11 groups (5 rats/group) to examine the toxicity of the prepared nanoparticles. Some hematological, biochemical parameters and apoptotic markers were evaluated. The findings revealed that injected AgNPs caused toxicity in both liver and kidney, as shown in the activity of the liver enzymes and kidney function. Treatment with PEE biosynthesized AgNPs injection ameliorated the harmful in hematological, biochemical parameters and liver homogenate genotoxicity induced by AgNPs toxicity, which was observed histopathologically. These results concluded that natural products and their NPs biosynthesis strategies can be exploited as a green chemistry approach, one-step, cost-effective, and eco-friendly for producing stable AgNPs on a large scale that have the potential to alleviate the alternation in the hematology, biochemical parameters and genotoxicity induced by AgNPs toxicity. This approach supports the dual purpose of natural product management.

Keywords: Genotoxicity, Green synthesis, Kidney function, Liver function, Nanoparticles toxicity, Pomegranate, Silver nanoparticles.

1. Introduction

Nanotechnology is a dynamic and expanding area, generating distinctive nanomaterials extensively utilized in biotechnology and nanomedicine applications. Biological synthesis of these nanomaterials provides a straightforward, safe, and dependable method, offering a more eco-friendly substitute for expensive and dangerous chemical procedures **[1]**. Compared to their chemically synthesized counterparts, these biologically synthesized nanomaterials show improved biocompatibility. They don't include any of the hazardous impurities that are usually created during chemical synthesis. Furthermore, organisms or their metabolites can serve as capping and stabilizing agents, negating the need for extra stabilizing agents during biosynthesis **[2,3]**. Because of their ease of use, safety, scalability, and promise for recycling agro-industrial waste, this biological approach, in particular, the synthesis of metal nanoparticles like silver, copper, gold, and others using plant extracts or waste, is gaining popularity **[4,5]**. Compared to traditional approaches, the sustainable synthesis of metal nanoparticles has numerous advantages, including simplicity, cost-effectiveness, accessibility, non-toxicity, and eco-friendly. This synthetic approach can also save a significant amount of energy at standard temperature and pressure. Root extract, seeds, leaf extract, stem extract, and fruit extract are among the plant components employed in this process; these components act as reducing and stabilizing agents **[6-8].**

As most *in vitro* investigations have shown, the cellular uptake of AgNPs is dependent on size, dosage, and coating. According to *in vivo* biodistribution investigations, Ag accumulation and toxicity to both nearby and distant organs have been documented after nanoparticles exposure. Even if the number of studies in this field has increased, more research is necessary to comprehend the mechanisms of toxicity following different AgNPs exposure modalities **[9]**.

Extract from pomegranates (*Punica granatum* L.) is high in phenolic compounds and phytochemicals, including flavonoids, tannins, anthocyanins, and polyphenols including punicalagin and ellagic acid. These substances have demonstrated potent reducing and antioxidant properties, which are essential for the biogenic synthesis of AgNPs and present a valuable resource for this green synthesis approach **[10,11].** Furthermore, the high tannin content of pomegranate extract can serve as a capping and reducing agent, enhancing the stability and biocompatibility of the produced AgNPs. Although the aforementioned plant extracts also include valuable bioactive components, pomegranate extract is a particularly appealing option for the environmentally friendly production of AgNPs with improved biological properties due to its special combination and high concentration of stabilizing and reducing agents **[12].** Pomegranate extracts can also control reduction and capping reactions

*Corresponding author e-mail: Mohamed_soliman@cu.edu.eg.; (Mohamed Abdel-Shakur Ali).

Received date 23 June 2025; Revised date 15 August 2025; Accepted date 26 August 2025

DOI: 10.21608/ejchem.2025.397161.11952

during the manufacture of AgNPs, producing more stable and tightly bound nanoparticles. For the synthesis of AgNPs, the biogenic pathway has a number of benefits over chemical reduction and photochemical methods **[13]**. The possible toxicity of the AgNPs can be decreased by stabilizing and lowering them using pomegranate extract **[14].** In general, This approach may serve as a basis for further studies and the development of novel treatments for cancer and infectious disorders **[15]**.

Hence, the aim of this study was to employ a simple, rapid and environmentally acceptable approach for green synthesis of AgNPs using pomegranate peel extract and starch as natural, cost-effective, and non-toxic reducing agents, which can serve as alternatives to hazardous chemical ones utilized in conventional chemical methods, such as sodium borohydride ($NaBH_4$). Overall, in this study, green synthesis of AgNPs using pomegranate extract was assessed to study the physical and chemical characteristics of NPs, evaluate their biologically eco-friendly properties, determine the antioxidant activity, and study the toxicity of NPs synthesized from pomegranate extract *in vivo*.

2. Materials and methods

2.1. Chemicals and materials

Silver nitrate ($AgNO_3$), Starch (ST), Sodium borohydride ($NaBrH_4$), and, 1, diphenyl-2-picryl hydrazyl (DPPH) were purchased from Sigma Co., but pomegranate fruit was collected from a local market in Giza, Egypt.

2.2. Preparation of pomegranate peel extract (PPE)

The pomegranate peels weighing 50g were washed repeatedly with distilled water to remove the dust and organic impurities, and then dried in an oven at 40 ºC. The peels were cut into small pieces, ground in to powder, and boiled with 250 mL of deionized water in a glass beaker under magnetic stirring for 30 min at 70 ºC. The extract was cooled down and filtered using Whatman No.1filter papers. The resultant filtrate was collected and stored at 4ºC until use **[6]**.

2.3. HPLC analysis of PPE phenolic and flavonoid compounds

Phenolic and flavonoid compounds were fractionated and detected by HPLC. Aqueous PPE was centrifuged at 10,000 x g for 10 min while being cooled and the supernatant was then filtered (size 0.22µm). Two mL of the filtrate were collected in a vial for auto-sampler injection into an HPLC Agilent (1260 series), which was outfitted with a solvent degasser, quaternary HP pump (Series 1100) and UV detector. The mobile phase including water (A) and 0.05% trifluoroacetic acid in acetonitrile (B) at a flow rate 0.9 ml/min, was sequentially programmed using the following linear gradient: 0 min (82% A); 0–5 min (80% A); 5-8 min (60% A); 8-12 min (60% A); 12-15 min (82% A); 15-16 min (82% A) and 16-20 (82%A). The injection volume was 5 µl for each of the sample solutions. The phenolic compounds were monitored at 280 nm and flavonoids at 330 nm using an Eclipse C18 column (4.6 mm x 250 mm i.d., 5 µm) maintained at 40 °C. Phenolic acid and flavonoid standards were dissolved in the mobile phase and injected into HPLC to calibrate tested samples against these standards based on retention time and peak area by the data analysis of HEWLLET Packed software **[2]**.

2.4. Green synthesis of AgNPs using PPE (PPE-AgNPs), starch (ST-AgNPs) and the mixture (PPE/ST-AgNPs)

$AgNO_3$ (1 mM, 50 mL) solution was added drop-wise to 10 mL of PPE, starch (5%) and 10 mL of the mixture (starch + PPE) solution (reducing and capping agents) under magnetic stirring at 700 rpm at 60 ºC for 30min. The mixture was protected from light during synthesis. pH was adjusted to 8 using 0.1 M NaOH and then incubated overnight at room temperature until the color of the mixture changed. Therefore, the reduction of Ag ions into AgNPs, followed by a change of color and formation of AgNPs, can be visually observed. To eliminate the unreacted agents, AgNPs dispersion was centrifuged for 15 min at 12000 rpm (Sorvall MTX 150, Thermo Fisher Scientific Inc.), washed several times with deionized water under centrifugation, followed by re-suspension in deionized water and kept at 4 °C until further use (Table 1) **[1]**.

2.5. Chemical synthesis of AgNPs using $NaBH_4$ ($NaBH_4$-AgNPs)

AgNPs were synthesized employing ice-cold $NaBH_4$ as a primary reductant agent to reduce the ionic silver and as a secondary stabilizing agent to stabilize the formed nanoparticles **[16,17]**. Thirty milliliters of freshly prepared aqueous solutions of $NaBH_4$ (0.002M) were added to an Erlenmeyer flask under magnetic stirring for 20 min with an ice bath, which was used to slow down the reaction and give better control over the final particle size/shape.$AgNO_3$ solution (1mM, 2 mL) was added drop-wise to $NaBH_4$ solution at 90 °C. Using 0.1 M NaOH, the pH of the solution was adjusted to 10.5 under continuous heating at 90°C and maintained for 20 minutes or until the alteration in color was noticeable. The prepared nano-sized particles were left to cool at ambient temperature. Therefore, the reduction of Ag ions into AgNPs, followed by a change of color and formation of AgNPs can be visually observed. To eliminate the unreacted agents, AgNPs dispersion was centrifuged for 15 min at 12000 rpm (Sigma, Germany), washed several times with deionized water under centrifugation, followed by re-suspension in deionized water and kept at 4 °C until further use (Table 1).

Table 1: Summarized synthesis protocol of AgNPs

Step	Green Synthesis Variants (PPE-AgNPs, ST-AgNPs, PPE/ST-AgNPs)	Chemical Synthesis ($NaBH_4$-AgNPs)
Precursor	1 mM, 50 mL added drop-wise	1 mM, 2 mL added drop-wise
Reducing/Capping Agents	10 mL of PPE, 10 mL of starch, or a 1:1 mixture of both (dual role as reducing and capping agents)	30 mL freshly prepared $NaBH_4$ (0.002 M) as primary reductant and stabilizer
Reaction Conditions	700 rpm, 60 °C, 30 min (light-protected), then incubated overnight at room temperature	Ice bath during initial mixing (20 min) to control nucleation, then heating at 90 °C for 20 min
pH Adjustment	Adjust to pH 8	Adjust to pH 10.5

2.6. Characterization of synthesized AgNPs

2.6.1. Visual observation and UV-VIS spectroscopy

The change of color was visually monitored to check the formation of AgNPs in a solution. Therefore, UV-Vis spectral analysis of synthesized NPs was performed to monitor the reduction of silver ions through a UV-VIS spectrophotometer (Thermo Scientific HERYIOS, England) at the scanning range of 300-700 nm with a resolution of one nm. The deionized water was used as a blank.

2.6.2. Particle Size and Zeta Potential

The mean hydrodynamic diameter with particle size range from 0.6 to 6000 nm and surface charge with zeta potential range from -200 to +200 mV of the synthesized NPs were performed using a Zetasizer Nano series (Nano ZS) particulate size description Analyzer (Malvern UK.)at scattering angle 90^{O} at room temperature. For three minutes, each measurement was captured through cumulative analysis to investigate the mean hydrodynamic diameter and the zeta potential.

2.6.3. Transmission electron microscopy (TEM)

The shape and size of produced NPs were determined using TEM (JEOL JEM-1400). A drop (2 µL) of NPs suspension was placed on a copper grid and utilized at a voltage of 200 kV.

2.6.4. Fourier transform infra-red spectroscopy (FTIR)

FTIR (Thermo Scientific NICOLET 380 FT-IR) was used to reveal the functional groups of synthesized AgNPs owing to their chemical structure by the potassium bromide (KBr) pellet method. Briefly, 2 mg of the samples were blended with 100 mg KBr, and then compacted to form a disc (3 mm in diameter). The absorption range of 400-4000cm^{-1} was used to capture the FTIR spectra of the tested samples.

2.7. Evaluation of antioxidant activity of PPE, PPE-AgNPs and PPE/ST-AgNPs by DPPH radical scavenging method

The antioxidant activity was measured by 1,1-diphenyl-2-picryl hydrazyl (DPPH) according to Sanganna *et al.* **[18]** with some modifications. Briefly, 0.1 mM of ethanolic DPPH solution was prepared. The PPE or its biosynthesized AgNPs were prepared in ethanol at various concentrations (0, 1.95, 3.9, 7.8125, 15.625, 31.25, 62.5, 125, 250, 500, 1000 µg/mL) by dilution [18]. Then 1 mL of ethanolic DPPH solution was mixed with 3 mL of PPE or its biosynthesized AgNPs solutions. The mixtures were shaken vigorously, allowed to stand at room temperature for 30 min, and then absorbance was measured spectrophotometrically at 517 nm. Ascorbic acid was used as a standard. The IC_{50} value of the tested samples was calculated using the Log Dose Inhibition Curve. IC_{50} is the concentration of the sample required to inhibit 50% of the DPPH free radical. A reaction mixture recorded a lower absorbance, indicating more and greater free radical activity. The experiment was done in triplicate. The percent DPPH scavenging effect was calculated as follows:

DPPH scavenging % (% inhibition) = $(A_0 - A_1 / A_0) \times 100$

Where A_0 was the absorbance of control reaction, and A_1 was the absorbance with the tested or standard sample.

2.8. *In vivo* Experiment

2.8.1. Ethics approval

This study protocol was performed in the Biochemistry Department, Faculty of Agriculture, Cairo University. The approval was carried out by the Institutional Animal Care and Use Committee (CU-IACUC) reviewers under ethical approval number CU11F2522**.**

2.8.2. Experimental animals

Fifty-five male albino Sprague-Dawley rats weighing 180 ± 20 g were supplied from the animal house of the National Research Centre, Dokki-Giza, Egypt. The animals were housed in the animal house of the Economic Entomology and Pesticide Department, in the Faculty of Agriculture, Cairo University in polyethylene cages at 25 ± 2 °C, 50-60% relative humidity and a light/dark cycle (12/12 h). The animals were adapted to free access to water and fed *ad libitium*on a basal diet for weeks adaptation period before the initiation of the experiment.

2.8.3. *In vivo* Experiment design

After a period of adaptation (two weeks), 55 of the experimental animals were divided into 11 groups (5 rats each) as follows: **Group (1)** was injected intraperitoneally (i.p.) with 200 µL sterile saline (normal control). **Group (2)** was injected i.p. with PPE (1 mg/kg b.w.). **Group (3)** was injected i.p. with PPE (5 mg/kg b.w.). **Group (4)** was injected i.p. with $NaBH_4$-AgNPs (1 mg/kg b.w.). **Group (5)** was injected i.p. with $NaBH_4$-AgNPs (5 mg/kg b.w.). **Group (6)** was injected i.p. with PPE -AgNPs (1 mg/Kg b.w.). **Group (7)** was injected i.p. with PPE -AgNPs (5 mg/Kg b.w.). **Group (8)** was injected i.p. with ST-AgNPs (1 mg/Kg b.w.). **Group (9)** was injected i.p. with ST -AgNPs (5 mg/Kg b.w.). **Group (10)** was injected i.p. with PPE/ST-AgNPs (1 mg/Kg b.w.). **Group (11)** was injected i.p. with PPE/ST-AgNPs (5 mg/Kg b.w.).The experimental feeding period continued for 12 weeks, and all groups were injected with every two consecutive days.

The chosen silver nanoparticle doses (1 mg/kg and 5 mg/kg) to provide significant biological effects within this dose range without causing extensive systemic toxicity or lethality. The doses were also supported by our pilot experiments in our laboratory performed before these studies, which validated their safety and biological relevance. To verify the sample size sufficiency, post hoc power analysis was conducted using G*Power software version 3.1. With 11 groups (n = 5 animals per group, total n = 55), with a medium effect size (f = 0.25) and α = 0.05, the statistical power was calculated to be approximately 0.84, which is considerably higher than the conventional value of 0.80. This confirms that the study was well powered to detect meaningful differences among treatment groups, and the design meets accepted preclinical toxicological study standards.

2.8.4. Collection of blood and tissue samples

After 12 weeks, the experimental animals were fasted overnight, decapitated, and blood samples of each rat were collected in dry-cleaned, sterilized and labeled centrifuge tubes. Serum was separated with centrifugation at 3000 x g for 5 min and kept at -20 ˚C until hematological and biochemical investigation. Organs of rats (liver, kidneys, spleen, lungs and testes) were taken for the determination of their weight. Liver tissues were taken, immersed in phosphate-buffered saline (PBS) solution (pH

7.4)and homogenized for genotoxicity investigation. Organs of rats (liver, kidneys and testes) were taken and immersed in 10% formalin solution for the histopathological examination.

2.8.5. Hematology and biochemical analysis

Complete blood capture (CBC) was evaluated automatically in all groups **[19]**, which include red blood cells (RBCs), white blood cells (WBCs), hemoglobin (Hb), hematocrit value (Hct), leucocyte count and platelets (Plt) **[20]**. Fasting blood glucose(FBG)level in serum was determined in all the studied groups using blood glucose meters and an autoanalyzer (glucose kit). Serum aspartate aminotransferases (AST) and Serum alanine aminotransferases (ALT) were assessed colorimetrically according to the method described by **Reitman and Frankel [21]** using GPL Kits, Barcelona, España. Serum alkaline phosphatase (ALP) activity was evaluated colorimetrically according to the method of **Belfield and Goldberg [22]**.

Serum total bilirubin levelwas measured colorimetricallyaccording to the method described by **Walter and Gerarde [23].** Serum urea level was measured according to the method described by **Fawcett and Scott [24]**, using Diamond Diagnostics kits, Egypt. Serum creatinine level was analyzed by the colorimetric procedure using Diamond Diagnostics kits, Egypt, according to **Houot [25].** Serum uric acid levelwasenzymatically carried out according to the method described by **Barham and Trinder [26].** Serum total protein was carried out according **to Gornall *et al.* [27].**Serum total albumin and Serum total globulin were performed according to **Doumas *et al*. [28].**

Serum triglycerides were determined colorimetrically according to the methods of **Fossati and Prencipe [29]** using the Diamond Diagnostics kit, Egypt. Serum total cholesterol was determined by the aquantitative –enzymatic- colourimetric method of **Allain *et al*. [30]** using Diamond Diagnostics kit, Egypt. Serum HDL- cholesterolwas determined according to **Grove [31]** by Diamond Diagnostics, kit, Egypt.Serum LDL- cholesteroland Serum vLDL -cholesterol were calculated according to **Friedewald *et al.* [32]** by using the Diamond Diagnostics kit, Egypt.

Genotoxicity examination was analyzed in liver tissue homogenate including BAX (Bcl-2-associated X protein), BCL-2 (B-cell lymphoma 2) and CASP-3 (Caspase 3).

2.8.6. Histopathological examination of liver, kidneys and testes

The liver, kidneys and testes of the sacrificed rats were eliminated and soaked in a 10% formalin solution. The tissue slides were then sheared washed and dehydrated in alcohol. These dehydrated sections were cleared in xylol, embedded in paraffin, sectioned at a thickness of 4-6 microns and stained with Hematoxylin and Eosin (H&E) for histopathological examination the study **[33]**.

2.9. Statistical analysis

The Costat program was used to perform the statistical analysis as mean ± standard deviation according to **Fisher [34].**In order to compare the significant differences between treatments means, the Least Significant Difference (LSD) test was employed **[35]**. Each value represents the mean of 5 rats (Mean ± SD). The same letters in each column represent the insignificant difference at $P<0.05$.

3. Results and discussion

3.1. HPLC analysis of PPE phenolic and flavonoid compounds

Pomegranate peels are an enriched source of functional ingredients including phenolic and flavonoid compounds. The HPLC analysis of the pomegranate peels for its phenolic compounds (Table 2) revealed the presence of 11 compounds in pomegranate peels. It was noticed that gallic acid, chlorogenic acid, catechin, methyl gallate, syringic acid, ellagic acid, vanillin, ferulic acid, naringenin, cinnamic acid and hesperidin were detected as shown in Table (2). Ellagic acid and gallic acid were the main functional ingredients with higher concentrations of about 41897.5 and 14645.9µg/g, respectively, comparable to other compounds.

Table 2: HPLC analysis of polyphenols and flavonoids of PPE

Compounds	Concentration (µg/g)
Gallic acid	14645.9
Cholorogenic acid	26.70
Catichin	5021.5
Methyl gallate	1206.16
Syringic acid	307.87
Ellagic acid	41897.5
Vanillin	81.18
Ferulic acid	56.12
Naringenin	114.13
Cinnamic acid	1672.16
Hesperedin	49.9

3.2. Characterization of synthesized AgNPs

3.2.1. Visual Observation and UV-VIS Spectroscopy

In the instance of a reaction mixture, the synthesis of AgNPs from $AgNO_3$ solution utilizing PPE, ST and $NaBH_4$ was completed rapidly. Since the mixture was exposed to stirring and heat for 30 min at room temperature and during incubation at room temperature overnight, the reduction of silver ions into AgNPs was commonly followed by a slow change of color from colorless or light yellow to reddish brown colloidal solution, indicating and monitoring the formation of AgNPs.The alteration of color during the reaction occurs due to the excitation of surface plasmon resonance in the AgNPs **[36]**.

Indicating the biogenic synthesis and the formation of AgNPs visually, the addition of $AgNO_3$caused a color shift from yellowish-orange to reddish-brown and furthermore, the adjustment of the pH to 8 led to a yellowish-black color **[37]**. Given its direct impact on size and form, this finding emphasizes the crucial role of pH in the synthesis of AgNPs **[38]**. Because of variations in ion density and diffusion rates, alkaline environments promote larger particles while acidic environments favor smaller ones**[39]**. Therefore, most likely, the employed pH range didn't significantly utilize the PPE's antioxidant degradation. PPE and ST with their hydroxyl abundance groups and their biocompatibility were used as reducing and capping agents.

Color perception of the chemicals involved is directly impacted by absorption in the visible range. Electronic transitions occur in molecules in this area of the electromagnetic spectrum. The formation of synthesized AgNPs in aqueous solution was confirmed using UV–VIS spectrophotometer analysis. The UV–VIS spectra of the prepared nano-formulations, along with their corresponding absorption peaks and wavelength are shown in Figure (1) and the scanning range for the sample was from 300 to 700 nm. The strong surface plasmon resonance band of AgNPs appears in the range of 440-480 nm **[40].**

Reaction mixtures of $AgNO_3$with PPE, ST, PPT/ST and $NaBH_4$ showed absorption peaks at 455,420, 420 and 460 nm, respectively, which are specific to AgNPs and a characteristic peak of AgNPs surface plasmon resonance the visible region **[41]**.These findings are similar to **Hassan *et al.* [42]**, who revealed that a strong peak was observed at 425 nm in pomegranate's silver bullet. Since AgNPs exhibited a characteristic peak in the spectrum at 425 nm, this indicated that the reduction procedure was effective. A higher number of NPs will produce a more considerable peak; hence the peak's intensity is an indication of the number of NPS generated. An increase in intensity might be interpreted as the formation of a greater number of NPs as a result of the reduction of $AgNO_3$ present in aqueous solutions during the reduction process.

Overall, the abrupt color shift and sharp, intense absorbance in the initial minutes of the process showed the capability of PE to produce ultra-fast nanoparticles. These results closely resemble those that have been reported in previous literature **[43].** AgNPs have garnered more attention due to their distinctive physicochemical properties and outstanding uses across numerous of domains, such as nanotechnology and healthcare **[44]**. The development of sustainable and environmentally friendly processes for AgNPs synthesis has garnered increasing attention in recent years **[45]**. As a more affordable and sustainable approach, the biogenic synthesis of AgNPs, which leverages biological sources including fungi, microbes, and plants as reducing and stabilizing agents, is one promising strategy **[46].** Thus, the biogenic synthesis of AgNPs from PPE was investigated *in vitro*. Prior research has investigated the synthesis of AgNPs utilizing a variety of plant extracts, including aloe vera, tea, and neem, indicating their potential for use in biomedical applications **[47]**. Nevertheless, these investigations frequently documented constraints on NPs, scalability, stability, and size uniformity. In contrast, this strategy using PPE, which is abundant in polyphenols, tannins, and other phytochemicals, facilitates a more monitored synthesis process to address these challenges and produce stable and uniform NPs. **Aly *et al.* [48]** showed the absorption intensity of biosynthesized AgNPs using commercial as well as the narrowness of the Ag-NPs Plasmon band, almost without affecting the maximum absorption peak of AgNPs at 430 nm.

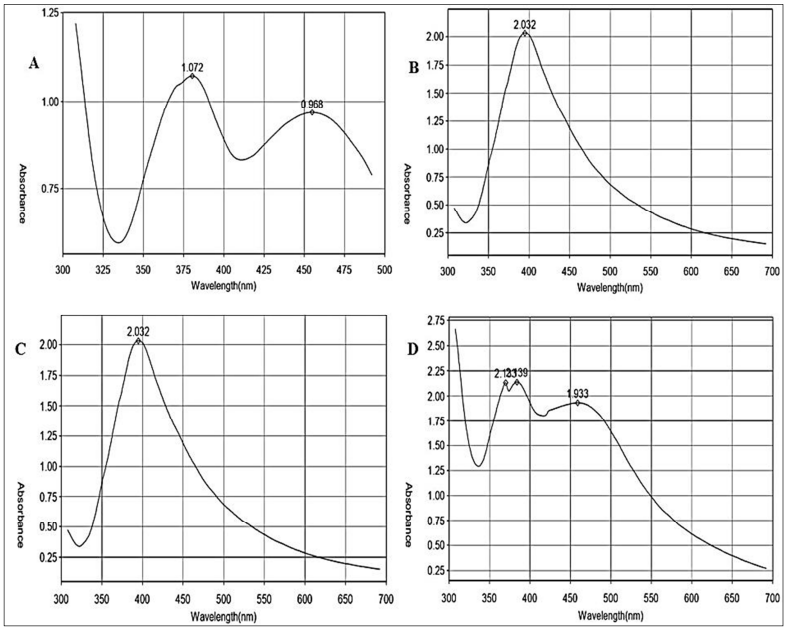

Figure 1: UV-VIS Spectroscopy of PPE-AgNPs (A), ST-AgNPs (B), PPE/ST-AgNPs (C) and $NaBH_4$-AgNPs (D).

3.2.2. Particle size and zeta potential

Dynamic light scattering (DLS) confirmed the size distribution of synthesized NPs, revealing mean diameters of 168.9, 139.6, 130.3 and 21.9 nm (Figures 2 A-D and Table 3), and Zeta potential of -7.74, -16.6, -18.2 and -22.4 mV (Figures 3 A-D and Table 3) for PPE-AgNPs, ST-AgNPs, PPE/ST-AgNPs and $NaBH_4$-AgNPs, respectively. This indicated a negative surface

charge, which indicates moderate stability, promoting electrostatic repulsion between particles to enhance the stability of the AgNPs. Zeta potential analysis was performed in order to analyze the surface potential and electrostatic stability of AgNPs in aqueous suspension. Higher negative surface charge NPs typically form stable colloids that disperse efficiently and show no evidence of aggregation. Particles with a negative zeta potential are negatively charged and repel one another, which stops them from aggregating. The NPs in suspension are kept stable by this repulsion, which also keeps them from settling out of the solution. According to zeta potential values for the biosynthesized pomegranate-AgNPs, **Hassan *et al.* [42]** found that zeta potential was −14.8 mV, which indicates moderate stability. For instance, the solutions with zeta potential above + 20 mV or below − 20 mV are stable. The relatively high negative zeta potential prevents aggregation between the particles and creates significant electrical double layer repulsion, which allows the zeta potential of the nanoparticles to signal the electrical surface properties of the particle.

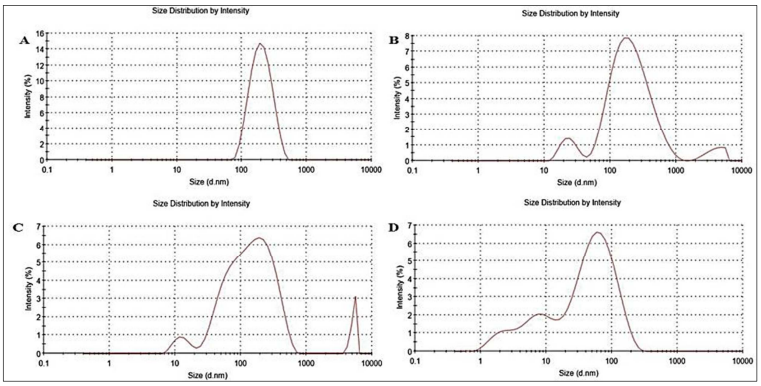

Figure 2: Particle size distribution of PPE-AgNPs (A), ST-AgNPs (B), PPE/ST-AgNPs (C) and $NaBH_4$–AgNPs (D).

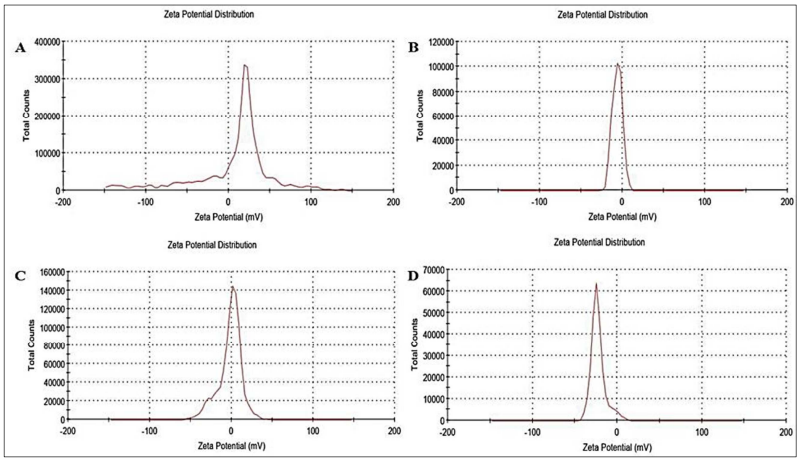

Figure 3: Zeta potential for PPE-AgNPs (A), ST-AgNPs (B), PPE/ST-AgNPs (C) and $NaBH_4$–AgNPs (D).

Table 3: PS (nm) and ZP (mV) for PPE-AgNPs, ST-AgNPs, PPE/ST-AgNPs and $NaBH_4$–AgNPs.

	PS (nm)	PDI	ZP (mV)
PPE-AgNPs	168.9	0.2	-7.74
ST-AgNPs	139.6	0.472	-16.6
PPE/ST-AgNPs	130.3	0.440	-18.2
$NaBH_4$–AgNPs	21.9	0.609	-22.4

- PS = particle size, PDI = polydispersity index, ZP = zeta potential

3.2.3. Transmission electron microscopy (TEM)

TEM analysis was displayed to show the morphology and size distribution of synthesized nanoformulations. All synthesized AgNPs were demonstrated mostly spherical shape (Figures 4 A-D), which indicated the completion of the NPs synthesis

process. According to TEM images, the synthesized AgNPs showed a consistent size distribution, suggesting that they were moderately aggregated and capable of retaining their original shape. The size diameter of synthesized NPs ranged from 9.63 to 49.0 nm. **Hassan *et al.* [42]** showed that TEM micrographs of the pomegranate-AgNPs showed a consistent size distribution, suggesting that they were not aggregated and capable of retaining their original shape. The particles were assessed to be in the typical size range of 20-25 nm. The spherical shape and distribution of pomegranate-AgNPs were also shown by the TEM micrograph, indicating the stability, reliability and appropriations of the synthesized NPs for utilization across numerous applications because it demonstrates that they are uniformly dispersed and of a suitable size and shape. As reported by **Yaqoob *et al.* [49]**, TEM analysis of AgNPs showed that they were spherical and cubic. The AgNPs' particle size range of 20 to 25 nm was also revealed by the TEM. Due to their high biocompatibility and ease of dispersion in aqueous solutions, AgNPs in this size range are perfect. Furthermore, AgNPs in this size range are very stable and readily applicable to a variety of biomedical applications **[50].**

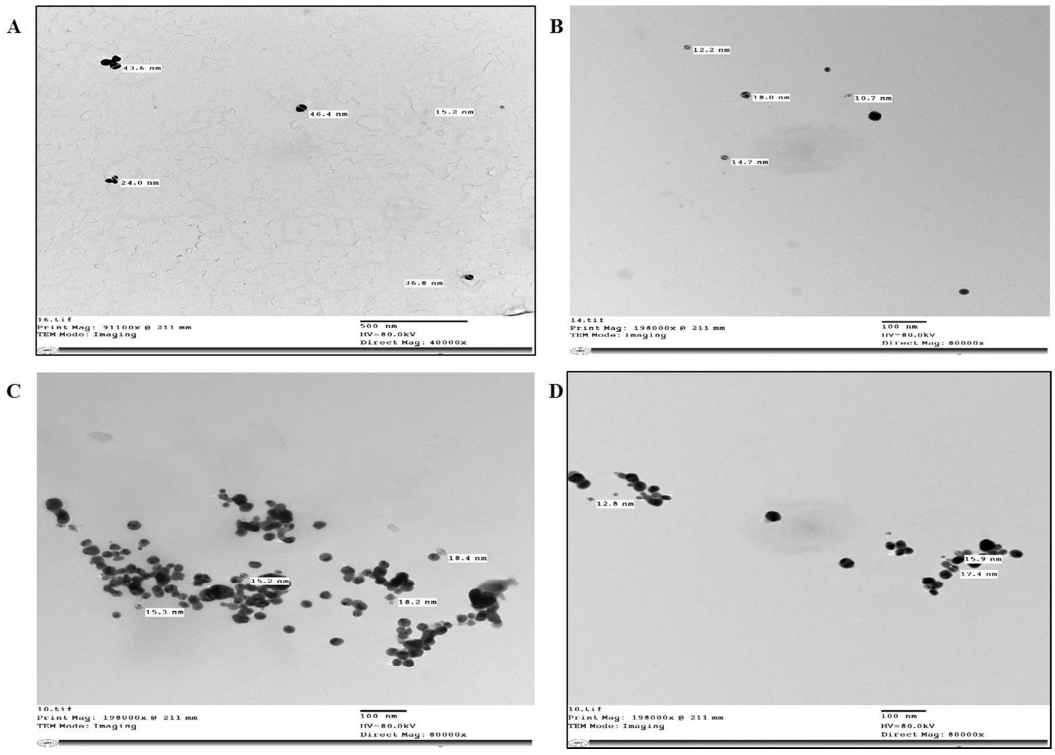

Figure 4: TEM micrograph of PPE-AgNPs (A), ST-AgNPs (B), PPE/ST-AgNPs (C) and $NaBH_4$–AgNPs (D).

3.2.4. Fourier transform infrared (FTIR)analysis of PPE and synthesized NPs

The existence of different functional groups in biomolecules that are in charge of bio-reducing Ag^+ and capping/stabilizing AgNPs was determined using FTIR measurements (Figures 5-9). The function groups were determined by comparing the observed intensity bands with standard values. FTIR spectrum displays absorption bands at 3286.13, 2906.54, 1715.13, 1602.10, 1333.55, 1221.26, 1144.91 and 1024.52 demonstrating that NPs include a capping agent (Figure 5). The absorption bands at 3286.13 cm^{-1} in spectra correspond to the O-H stretching vibration, demonstrating the presence of alcohol and phenol. The peak at 1602.10 corresponds to the C=O stretching vibration of carbonyls **[51]**. Results of the FTIR study of biosynthesized AgNPs using PEE showed absorption peaks At 3278.40, 2935.29, 1717.76, 1606.35, 1190.69 and 1016.89 cm^{-1} (Figure 6). The absorption peaks were assigned to free hydroxyl groups or phenolic hydroxyl, C–H of alkanes, O–H of alcohol or N–H of amines, C=O of carboxylic acid or ester, O–C stretching, C-N of aliphatic amines or alcohol/phenol and aromatic C-H, respectively. Results of the FTIR study of biosynthesized AgNPs using ST showed absorption peaks at 3266.00, 2925.11, 1600.89, 1334.87, 1148.74 and 1010.22 cm^{-1} (Figure 7). The absorption peaks were assigned to free hydroxyl of alcohol or phenol, O–H of alcohol or N–H of amines, C–H of alkanes, O–C stretching, C=O of carboxylic acid or ester, hydroxyl groups or phenolic hydroxyl, C-N of aliphatic amines or alcohol/phenol and aromatic C-H, respectively .Absorption band was observed at 3266.00cm^{-1} indicating the O–H stretching of ST. The C-H band showed asymmetric stretching at 2925.11 cm^{-1}, while the water adsorbed in the amorphous area of ST was responsible for the band at 1600.89 cm^{-1}. The distinctive band that appeared at 1010.22cm^{-1} was due to C–O–H bending of ST. In addition, the peaks in the ST-capped NPs were broader and longer than in ST alone, suggesting this may be because of intra- and intermolecular hydrogen bonds. The effective OH group of the ST capping agent is successfully bound to the AgNPs, as confirmed by the ST characteristic bands exhibited in the synthesized NPs.Results of the FTIR study of biosynthesized AgNPs using PEE and ST showed absorption peaks at 3723.43, 3263.35, 1729.44, 1635.98, 1328.31 and 993.39 cm^{-1} (Figure 8). The absorption peaks

were assigned to free hydroxyl of alcohol or phenol, O–H of alcohol or N–H of amines, C–H of alkanes, O–C stretching, C=O of carboxylic acid or ester, hydroxyl groups or phenolic hydroxyl, C-N of aliphatic amines or alcohol/phenol and aromatic C-H, respectively. Results of the FTIR study of biosynthesized AgNPs using $NaBH_4$ showed absorption peaks at 3339.88, 2874.66, 1650.59, 1650.59, and 1345.64 cm^{-1} (Figure 9). The absorption peaks were assigned to O–H, C–H, O–C stretching and N=-O, respectively. All these results indicated that AgNPs were attached to the functional groups presented in PPE and ST. The silver atom and the electron-rich groups (oxygen/carbonyls) found in PPE and ST created a coordination bond, which caused the peak to shift and an increase in bond length and frequency.

The FTIR analysis of pomegranate-AgNPs showed that the extracellularly synthesized pomegranate extract produced firm peaks at 2953.36 cm^{-1}, 1651.33 cm^{-1}, 1423.10 cm^{-1}, 224.72 cm^{-1}, 1046.89 cm^{-1}, 931.42 cm^{-1}, 645.29 cm^{-1}, and 571.06 cm^{-1}. These peaks were ascribed to the carbonyl (C=O), amide I, amide II, O–H stretching, C–H stretching, C-N stretching, C-O stretching, and C-OC stretching vibrations **[52]**, respectively. Moreover, the Ag-O bond is also responsible for the peak at 2953.36 cm^{-1}, while the Ag-N bond is responsible for the peak at 1651.33 cm^{-1} **[53].** The FTIR spectrum of the pomegranate-AgNPs indicated that the extract's phytoconstituents have effectively contributed to the production and functionalization of AgNPs **[54]**. Pomegranate extract has been shown to contain flavonoids and polyphenols in preliminary research. The finding lends evidence to the hypothesis that flavonoids and polyphenols contribute in the fabrication of AgNPs **[55]**. The formation and stabilization of AgNPs are significantly influenced by these polyphenols and flavonoids.

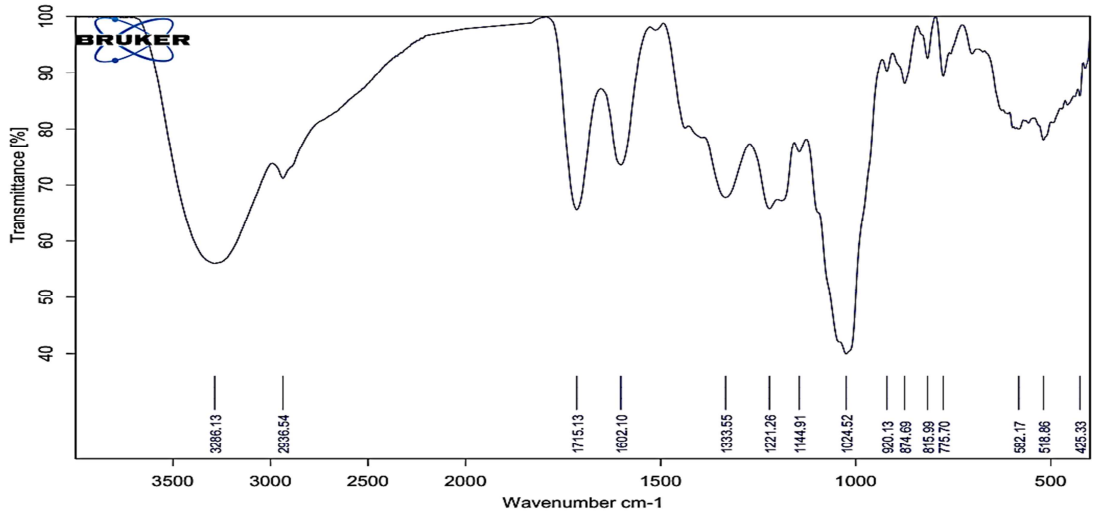

Figure 5: FT-IR spectrum of PPE.

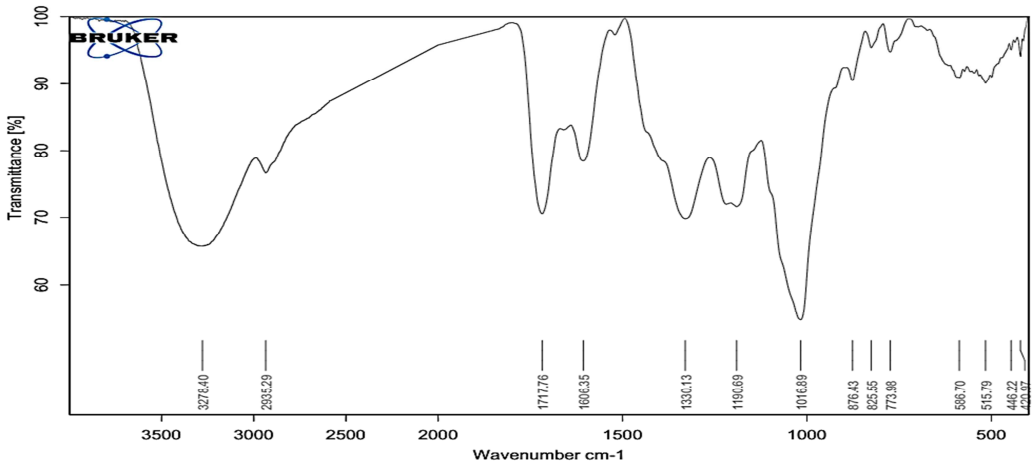

Figure 6: FT-IR spectrum of PPE-AgNPs.

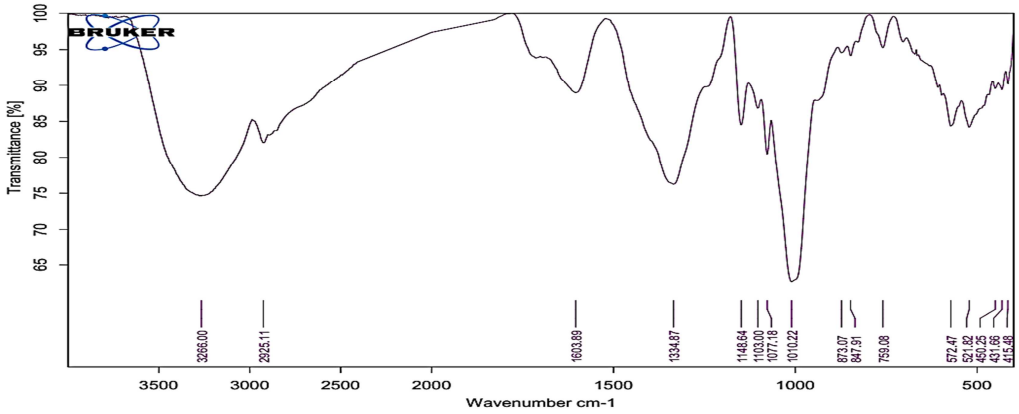

Figure 7: FT-IR spectrum of ST-AgNPs

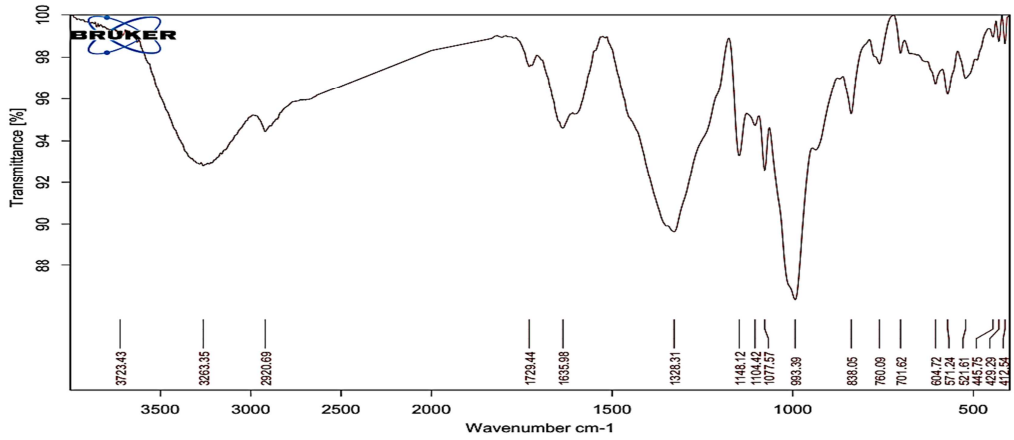

Figure 8: FT-IR spectrum of PPE/ST–AgNPs.

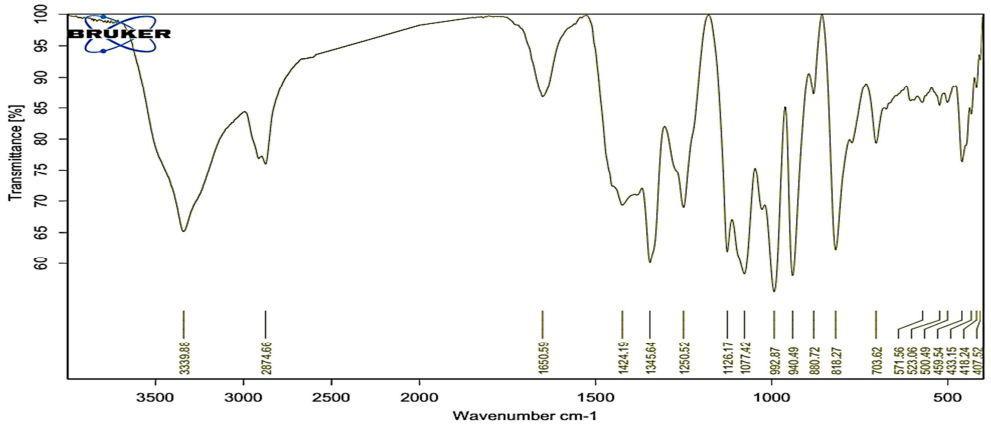

Figure 9: FT-IR spectrum of $NaBH_4$-AgNPs.

3.3. Antioxidant activity of PPE, PPE-AgNPs and PPE/ST-AgNPs by DPPH radical scavenging

The DPPH radical scavenging activity of PPE and its biosynthesized AgNPs compared to ascorbic acid as a standard was displayed in Table (4). The results confirmed that the PPE and its biosynthesized AgNPs have free radical scavenging. There was a dose-dependent increase in antioxidant activity as the concentration increased. The PPE, PPE-AgNPs and PPE/ST-AgNPs at various concentrations (1.95-1000 µg/mL) displayed antioxidant activity of 41.8% to 98.4%, 41.8% to 96.9% and 7.7% to 60% with an average IC_{50} value of 3.91, 4.28 and 391.14 µg/mL, respectively. The PPE-AgNPs exhibited higher

scavenging activity of DPPH of the prepared nanoparticles (IC_{50} value 4.28 µg/mL) about similar the standard ascorbic acid (IC_{50} value 4.08 µg/mL) but not higher than PPE which exhibited scavenging activity of DPPH (IC_{50} value 3.91 µg/mL) similar of the standard ascorbic acid (IC_{50} value 4.08 µg/mL). The percentage of DPPH that is decreased by a known quantity of sample extract is a measure of the ability of the plant extract to scavenge free radicals. The response between a particular antioxidant and a stable free radical, such as DPPH, is fascinating in the DPPH assay. In this study, it could be noticed that PPE and its biosynthesized AgNPs had a great free radical scavenging activity and showed a significant increase in the percent DPPH inhibition compared to the control, which the least scavenging activity. This activity is probably due to the extract's high phenolic component concentration, especially its flavonoid content. These results demonstrate its potential as a natural antioxidant source. According to recent research, PPE has a wider range of uses than just antioxidants. It is effective as a multifunctional agent that can be used as a reducing, capping, and stabilizing agent during metal nanoparticle synthesis **[53].** DPPH provides a simple and rapid assessment and is widely used to determine the antioxidant activity of compounds or nanoparticles. Compared to ordinary reference ascorbic acid, PPE/ST-AgNPs have lower antioxidant activity because the presence of starch in the nanoparticles structure may affect the scavenging activity by coating the function groups of plant extract and the aggregation effect on the nanoparticles activity (Figure 4C). Ascorbic acid showed a greater scavenging activity (IC_{50} 4.08 µg/mL) than PPE/ST-AgNPs, which had a larger IC_{50} value (391.14 µg/mL). Compared to ascorbic acid (IC_{50} 32.6±14.8 µg/mL), the synthesized AgNPs, which had a larger IC_{50} value (61.81±19.4 µg/mL) demonstrated a weaker scavenging activity **[56].** The use of antioxidants for alleviating oxidative stress is becoming more prevalent, and natural antioxidants are increasingly common compared to synthetic ones. Pomegranate-AgNPs are enriched antioxidant sources ready to go into the tissues, given their ability to easily and rapidly penetrate deep down into the tissues. AgNPs are an efficient scavenger of free radicals, particularly those based on oxygen. Oxidation-reduction processes are used to produce metallic nanoparticles from precursor salts. The reducing agents included in plant extracts cause the electrons to migrate to the metal precursor's ions, generating NPs **[57]**. The synthesis of AgNPs from plants is more advantageous compared to microorganisms and algae, since it eliminates the time-consuming steps involved in cultivating the cultures on media, making it less biohazardous and easily enhanced **[58]**. **Tyagi *al.* [59]** indicated that the antioxidant potential was dose-dependent in both AgNPs and the extract. Also, **Erenler and Dag [60]** revealed that the DPPH scavenging ability was significant with the IC_{50} of 12.25 mg mL^{-1} of the biosynthesized AgNPs but higher than the IC_{50} of the plant extract (IC_{50} 21.66 mg mL^{-1}).

Table 4: DPPH scavenging% of PPE, PPE-AgNPs and PPE/ST-AgNPs comparable with ascorbic acid (standard)

	DPPH scavenging %										
Concentrations (ug/mL)	**1000**	**500**	**250**	**125**	**62.5**	**31.25**	**15.625**	**7.8125**	**3.9**	**1.95**	**IC_{50} (ug/mL)**
Ascorbic acid	97.0	94.5	92.7	86.4	78.0	71.2	64.2	56.3	45.8	41.7	4.08
PPE	98.4	96.5	92.2	84.8	78.1	71.4	64.6	57.2	47.5	41.8	3.91
PPE-AgNPs	96.9	94.8	90.8	83.1	77.1	70.5	63.5	54.9	46.7	41.8	4.28
PPE/ST-AgNPs	60.0	52.6	46.3	38.8	32.2	28.5	24.1	17.7	12.5	7.7	391.14

3.4. Body weight, body weight gain, food intake and feed efficiency of the experimental animals

The data presented in Table (5) showed that the initial body weights of all groups were non-significantly different, however, after 12 weeks of the initial period; body weight gain was significantly lower in $NaBH_4$-AgNPs (5 mg), PPE -AgNPs (1 mg), PPE/ST-AgNPs (1 mg) and PPE/ST-AgNPs (5 mg) groups as compared to other groups. The gain in body weight at the end of the experimental period for the normal control group was 233 g, while PPE (5 mg), $NaBH_4$-AgNPs (5 mg), PPE-AgNPs (1 mg), PPE/ST-AgNPs (1 mg) and PPE/ST-AgNPs (5 mg) groups were212, 113, 113, 176 and 197 g, respectively. These results showed that these applied treatments may have negative effect on feed efficiency which was 4.7% for PPE (5 mg), 5.1% for $NaBH_4$-AgNPs (5 mg), 5.1% for PPE-AgNPs (1 mg), 8.1% for PEE/ST-AgNPs (1 mg) and 5.8% for PPE/ST-AgNPs (5 mg) as compared to other groups. On the other hand, PPE (1 mg), $NaBH_4$-AgNPs (1 mg), PPE-AgNPs (5 mg) and ST-AgNPs (5 mg) groups showed a higher Increase in body weight gain compared to the normal control group which was 240, 303, 275 and 297 g, respectively. These results hypothesized that these applied treatments may have non-significant differences in feed efficiency and weight gain.

Table 5: Body weight, body weight gain,food intake and feed efficiency of the experimental animals

Treatment	**Initial body weight (g)**	**Final body weight (g)**	**body weight gain (g)**	**Food intake (g)**	**Feed efficiency (%)**	**Relative to control (%)**
Group (1)	187±2.1	420±1.3	233±1.1^{b}	2155	10.8	100
Group (2)	176±3.2	416±0.5	240±1.0^{b}	2175	11.0	102
Group (3)	180±2.1	392±1.5	212±1.6^{b}	2180	4.7	90
Group (4)	181±3.5	484±0.2	303±0.4^{a}	2150	14.0	130
Group (5)	183±2.4	296±0.1	113±0.2^{d}	2197	5.1	47
Group (6)	186±2.5	299±1.7	113±1.3^{d}	2187	5.1	48
Group (7)	177±3.3	452±1.3	275±0.9^{ab}	2180	12.6	117

Group (8)	188±2.01	414±1.4	226±0.8^{b}	2177	10.3	95
Group (9)	175±3.1	454±0.3	297±0.9^{a}	2187	13.5	125
Group (10)	183±3.19	359±0.2	176±0.4^{c}	2176	8.1	75
Group (11)	185±3.4	312±1.1	197±0.7^{d}	2189	5.8	54

Each value represents the mean of 5 rats (Mean ± SD). The same letters in each column represent the insignificant difference at P<0.05. Group (1): control; group (2): PPE (1 mg); group (3): PPE (5 mg); group (4): $NaBH_4$-AgNPs (1 mg); group (5): $NaBH_4$-AgNPs (5 mg); group (6): PPE-AgNPs (1 mg); group (7): PPE-AgNPs (5 mg); group (8): ST-AgNPs (1 mg); group (9): ST-AgNPs (5 mg); group (10): PPE/ST-AgNPs (1 mg) and group (11): PPE/ST-AgNPs (5 mg).

3.5. Liver weight and kidney weights of the experimental rats

Table (6) shows the liver and kidney weights of animals in each group. In the experimental period, animals treated with PPE-NPs (1 mg) and PPE/ST-NPs (5 mg) significantly decreased their liver weights, which were 4.62±0.8 g (ratio 2.48%) and 4.12±0.5 g (ratio 2.22 %), respectively, when compared with the normal control group, 5.54±0.2 g (ratio 2.70 %). The weight value of kidneys was 1.46±0.3 g (ratio 0.70%) for the normal control group, but the value was significantly decreased for the PPE/ST-NPs (5 mg) group, which was 1.06±0.2 g (ratio 0.57 %). The other groups didn't have non-significant differences compared to the normal control group. The decrease in liver weight (4.62 ± 0.8 g, ratio 2.48%, and 4.12 ± 0.5 g, ratio 2.22%) when compared to controls (5.54 ± 0.2 g, ratio 2.70%) may be indicative of a hepatocellular response to nanoparticle exposure. While small decreases in liver weight may indicate reduced metabolic activity or reversible hepatocellular contraction, they might also result from subclinical toxicity or perturbed protein synthesis **[61]**. Nevertheless, as there were no gross findings of systemic toxicity and other groups received no significant alterations, these findings could be a result of dose-dependent metabolic adaptation and not irreversible liver damage. Similarly, the reduction in kidney weight within the PPE/ST-NPs (5 mg) group (1.06 ± 0.2 g, ratio 0.57%) with respect to controls (1.46 ± 0.3 g, ratio 0.70%) is significant. Kidney is a primary clearance organ for nanoparticles, and weight losses may reflect changes in renal perfusion or earliest evidence of nephron involvement rather than frank structural damage **[62]**. Nevertheless, the absence of analogous changes in the other treatment groups suggests that the response is formulation- and dose-dependent rather than a general feature of all PPE-based nanoparticles. The absence of substantial weight loss in the majority of groups is in agreement with previous reports indicating that biologically synthesized silver nanoparticles have comparatively low subacute toxicity against their chemically synthesized analogs **[63]**. Yet, in the absence of supportive histopathological or biochemical evidence, it cannot be ascertained if the weight losses are simply benign physiological adaptation or initial organ stress.

Table 6: Liver weight, kidneys weight and the ratio relative to animal body weight

Treatment	Initial body weight	Kidneys weight	Ratio	Relative to control	Liver weight	Ratio	Relative to control
	G	G	%	%	g	%	%
Group (1)	203±2.5	1.46±0.3^{b}	0.70	100	5.54±0.2^{b}	2.70	100
Group (2)	176±0.5	1.35±0.3^{ab}	0.76	108	5.07±0.1^{ab}	2.90	107
Group (3)	180±1.5	1.44±0.7^{a}	0.80	114	5.45±0.1^{a}	3.02	114
Group (4)	181±0.2	1.38±0.2^{ab}	0.76	108	4.95±0.8^{b}	2.73	101
Group (5)	183±0.1	1.49±0.3^{a}	0.81	115	5.27±0.1^{ab}	2.87	106
Group (6)	186±1.7	1.36±0.6^{ab}	0.73	104	4.62±0.8^{c}	2.48	91
Group (7)	177±1.3	1.35±0.5^{ab}	0.76	108	5.05±0.3^{ab}	2.85	105
Group (8)	188±1.4	1.32±0.6^{b}	0.70	100	4.84±0.5^{bc}	2.57	95
Group (9)	175±0.3	1.34±0.2^{ab}	0.76	108	4.45±0.3^{bc}	2.54	94
Group (10)	183±0.2	1.30±0.7^{b}	0.71	101	5.42±0.8^{a}	2.96	109
Group (11)	185±1.1	1.06±0.2^{c}	0.57	81	4.12±0.5^{b}	2.22	82

Each value represents the mean of 5 rats (Mean ± SD). The same letters in each column represent the insignificant difference at P<0.05. Group (1): control; group (2): PPE (1 mg); group (3): PPE (5 mg); group (4): $NaBH_4$-AgNPs (1 mg); group (5): $NaBH_4$-AgNPs (5 mg); group (6): PPE-AgNPs (1 mg); group (7): PPE-AgNPs (5 mg); group (8): ST-AgNPs (1 mg); group (9): ST-AgNPs (5 mg); group (10): PPE/ST-AgNPs (1 mg) and group (11): PPE/ST-AgNPs (5 mg).

3.6. Spleen, lungs and testes weights of the experimental rats

The results reported in Table (7) showed the spleen, lungs and test weights of rats in each group. In the study period, animals administered with PPE alone (1 mg and 5 mg), $NaBH_4$-AgNPs (1 mg and 5 mg), PPE-AgNPs (1 mg and 5 mg), ST-AgNPs (1 mg and 5 mg) and PPE/ST-NPs (1 mg and 5 mg) were significantly decreased in their spleen weights when compared to the normal control group. The weight value of the spleen was 1.03±0.1 g (ratio 0.50%) for the normal control group but the value was decreased for other groups which were 0.75±0.3 g (ratio 0.42%), 0.62±0.4 g (ratio 0.34%), 0.79±0.3 g (ratio 0.43%), 0.73±0.1 g (ratio 0.39%), 0.78±0.3 g (ratio 0.41%), 0.68±0.3 g (ratio 0.38%), 0.67±0.2 g (ratio 0.35%), 0.70±0.3 g (ratio 0.40%), 0.80±0.5 g (ratio 0.43%) and 0.64±0.6 g (ratio 0.34%), respectively. The weight value of the lungs was 1.12±0.7 g (ratio 0.55%) for normal control group but the value was non-significantly increased for PPE (1 mg and 5 mg), $NaBH_4$-AgNPs (1 mg and 5 mg), PPE-AgNPs (1 mg), ST-AgNPs (1 mg and 5 mg), PPE/ST-AgNPs (1 mg and 5 mg) groups which were 1.27±0.4 g (ratio 0.72%), 1.23±0.5 g (ratio 0.68%), 1.16±0.2 g (ratio 0.64%), 1.32±0.5 g (ratio 0.72%), 1.11±0.2 g (ratio 0.60%), 2.26±0.3 g (ratio 0.67%), 1.30±0.4 g (ratio 0.74%), 1.30±0.4 g (ratio 0.71%) and 1.25±0.6 g (ratio 0.67%), respectively. On the other hand, the value was significantly increased for the PPE-AgNPs (5 mg) group which was 2.21±0.2 g (ratio 1.24%). The weight value of tests was 4.35±0.5 g (ratio 2.14%) for normal control group but the value was non-significantly increased for PPE (1 mg), $NaBH_4$-AgNPs (5 mg), PPE-AgNPs (1 mg) and PPE/ST-AgNPs (1 mg and 5 mg) groups, which were 4.02±0.4 g

(ratio 2.28%),4.17±0.4 g (ratio 2.27%), 4.02±0.3 g (ratio 2.16%), 3.81±0.2 g (ratio 2.14%) and 3.63±0.2 g (ratio 1.96%). The value was significantly increased in test weight of PPE (5 mg), $NaBH_4$-AgNPs (1 mg), PPE-AgNPs (5 mg), ST-AgNPs (1 mg) and ST-AgNPs (5 mg) when compared to the normal control group.

The results in Table (7) revealed a significant decrease in spleen weight in all the treatment groups, suggesting a generalized effect of PPE, $NaBH_4$-AgNPs, PPE-AgNPs, ST-AgNPs, and PPE/ST-AgNPs on immune organ cellularity, which may be a reflection of mild immunomodulation rather than frank toxicity. The finding agreed with available evidence that silver nanoparticles would tend to accumulate in the spleen and influence lymphoid tissue architecture. Lung weights were largely unaffected compared to controls, the only exception being the notable increase in the PPE-AgNPs (5 mg) group, which indicates localized pulmonary accumulation or an inflammatory response at the higher dose, consistent with literature accounts of nanoparticle deposition in pulmonary tissue. Testis weights were significantly elevated in several groups, justifying the need for reproductive toxicity testing as nanoparticles have been shown to cross the blood–testis barrier and induce oxidative stress or functional alterations in reproductive tissues. Collectively, these changes in organ weights emphasize the necessity for supporting investigations, including histopathology, biochemical examination, and biodistribution studies, to determine whether such changes are indicative of transient physiological adaptation or early morphological manifestations of organ-specific toxicity **[62,64]**.

Table 7: Spleen weight, lungs weight, testes weight and the ratio relative to animal body weight

Treatment	Initial body weight	Spleen weight	Ratio	Relative to control	Lungs weight	Ratio	Relative to control	Testes weight	Ratio	Relative to control
	G	G	%	%	g	%	%	g	%	%
Group (1)	203±2.5	1.03±0.1^{a}	0.50	100	1.12±0.10^{d}	0.55	100	4.35±0.40^{c}	2.14	100
Group (2)	176±0.5	0.75±0.03^{b}	0.42	84	1.27±0.04^{b}	0.72	130	4.02±0.40^{c}	2.28	106
Group (3)	180±1.5	0.62±0.04^{c}	0.34	68	1.23±0.05^{bc}	0.68	123	4.37±0.37^{b}	2.42	113
Group (4)	181±0.2	0.79±0.03^{b}	0.43	86	1.16±0.10^{c}	0.64	116	4.29±0.40^{bc}	2.37	110
Group (5)	183±0.1	0.73±0.06^{bc}	0.39	78	1.32±0.05^{b}	0.72	130	4.17±0.40^{c}	2.27	106
Group (6)	186±1.7	0.78±0.07^{b}	0.41	82	1.11±0.10^{cd}	0.60	109	4.02±0.30b^{c}	2.16	100
Group (7)	177±1.3	0.68±0.06^{bc}	0.38	76	2.21±0.20^{a}	1.24	225	4.89±0.40^{a}	2.76	128
Group (8)	188±1.4	0.67±0.04^{c}	0.35	70	2.26±0.20^{bc}	0.67	121	4.91±0.20^{ab}	2.61	121
Group (9)	175±0.3	0.70±0.05^{b}	0.40	80	1.30±0.12^{b}	0.74	134	4.41±0.30^{b}	2.52	117
Group (10)	183±0.2	0.80±0.05^{b}	0.43	86	1.30±0.13^{b}	0.71	129	3.81±0.20^{cd}	1.09	97
Group (11)	185±1.1	0.64±0.06^{c}	0.34	68	1.25±0.11^{bc}	0.67	121	3.63±0.20^{d}	1.96	91

Each value represents the mean of 5 rats (Mean ± SD). The same letters in each column represent the insignificant difference at $P<0.05$. Group (1): control; group (2): PPE (1 mg); group (3): PPE (5 mg); group (4): $NaBH_4$-AgNPs (1 mg); group (5): $NaBH_4$-AgNPs (5 mg); group (6): PPE-AgNPs (1 mg); group (7): PPE-AgNPs (5 mg); group (8): ST-AgNPs (1 mg); group (9): ST-AgNPs (5 mg); group (10): PPE/ST-AgNPs (1 mg) and group (11): PPE/ST-AgNPs (5 mg).

3.7. Biochemical analysis

3.7.1. Liver function of the experimental animals

Because the majority of oral medications and xenobiotics are toxic to the liver, the liver is a key target organ. Effects of synthesized AgNPs on liver function were determined, and the results were summarized in Table (8).The results showed that the PPE (1 mg) administration alone significantly increased the activities of AST, ALT, AST/ALT ratio and bilirubin content but significantly decreased the activity of ALP in the serum of PPE group(1 mg) as compared to the normal control group. The administration of the PPE (5 mg) significantly decreased the activities of ALT and ALP but significantly increased the AST activity, AST/ALT ratio and non-significantly increased the content of bilirubin in comparison with the normal control. Animals administered with $NaBH_4$-AgNPs (1 mg) significantly increased the activities of AST, ALT, AST/ALT ratio and bilirubin content but significantly decreased the activity of ALP when compared to the normal control group. Administration of $NaBH_4$-AgNPs (5 mg) significantly increased the activities of AST, ALT, ALP and bilirubin content, but significantly decreased the AST/ALT ratio as compared to the normal control. As for the PPE-AgNPs (1 mg) group, significant changes with an increase in the activities of AST, ALT and bilirubin content were observed but significantly decreased the AST/ALT ratio and ALP activity as compared to the normal control. Administration of the PPE-AgNPs (5 mg) exhibited a significant reduction in the AST/ALT ratio and ALP activity and significantly increased the activities of AST, ALT, ALP and bilirubin content as PPE-AgNPs (1 mg) group when compared to the normal control group. A significant increase was observed in the activities of AST, ALT and bilirubin content but significant reduction in the ALP activity and non-significant changes in AST/ALT ratio when ST-AgNPs (1 mg) was compared to the normal control. ST-AgNPs (5 mg) group revealed a significant increase in the activities of AST, ALT and bilirubin content, but a significant reduction in the ALP activity and non-significant changes in the AST/ALT ratio as ST-AgNPs (1 mg) when compared to the normal control group. The administration of PPE/ST-AgNPs (1 mg)

significantly increased the activity of AST, AST/ALT ratio and the content of bilirubin but significantly decreased the ALT and ALP activities as PPE (5 mg) when compared to the normal control, on the otherwise, PPE/ST-AgNPs (5 mg) significantly increased the activities of AST, ALT, AST/ALT ratio and the content of bilirubin but significantly decreased the ALP activity compared to normal control group.

The liver enzyme profile as presented in Table 6 demonstrates that both the plant extract (PPE) and chemically ($NaBH_4$) or biotransduced synthesized AgNPs (PPE, ST, PPE/ST) caused dose-dependent hepatocellular effects as evident from the alteration of serum transaminases, ALP activity, and bilirubin level. AST, ALT, and bilirubin elevations in more than one treatment group indicate potential hepatocellular injury or metabolic strain, in line with previous research to prove that silver nanoparticles can induce alterations of hepatic enzyme homeostasis and oxidative damage **[65]**. Variable but significant alterations in AST/ALT ratio reflect differential trends of hepatocellular injury, where some of the samples (e.g., PPE/ST-AgNPs at 1 mg) showed mixed hepatocellular and cholestatic patterns, whereas others (e.g., $NaBH_4$-AgNPs at 5 mg) showed more uniform elevation of the enzymes. ALP reduction observed in different groups could be suggestive of inhibition of membrane-bound enzyme systems or enhanced damage to the bile canaliciuli function, and ALP increase in $NaBH_4$-AgNPs (5 mg) could be suggestive of dose-related cholestasis. These results agree with earlier reports indicating that surface chemistry of nanoparticles, capping, and route of synthesis play a significant role in hepatic uptake and toxicological profiles [66].

Table 8: Liver function of the experimental animals

Treatment	ALT (U/L)	AST (U/L)	AST/ALT	ALP (U/L)	Bilirubin (mg/dL)
Group (1)	12.02 ± 0.44^{a}	14.94 ± 1.32^{a}	1.18	244.66 ± 20.03^{a}	0.32 ± 0.04^{a}
Group (2)	12.24 ± 0.70^{b}	20.8 ± 1.46^{b}	1.7	169.82 ± 15.02^{b}	0.60 ± 0.02^{b}
Group (3)	9.78 ± 0.46^{c}	22.2 ± 1.43^{c}	2.26	58.8 ± 5.03^{c}	0.39 ± 0.02^{bc}
Group (4)	19.76 ± 0.78^{d}	37.8 ± 1.30^{d}	1.91	222.54 ± 20.03^{d}	0.78 ± 0.05^{bxd}
Group (5)	70.82 ± 4.21^{d}	56.3 ± 2.80^{d}	0.79	582.12 ± 40.11^{e}	1.7 ± 0.15^{bcd}
Group (6)	26.68 ± 1.50^{e}	17.16 ± 1.33^{e}	0.64	176.56 ± 10.14^{e}	0.44 ± 0.04^{bcd}
Group (7)	32.8 ± 1.79^{ee}	31.26 ± 1.36^{e}	0.95	201 ± 20.07^{f}	0.65 ± 0.03^{cd}
Group (8)	24.94 ± 1.26^{eg}	22.72 ± 1.93^{e}	0.91	146.18 ± 10.08^{g}	0.41 ± 0.03^{d}
Group (9)	40.46 ± 1.89^{eg}	42.5 ± 2.97^{e}	1.05	197.28 ± 10.11^{k}	0.64 ± 0.04^{d}
Group (10)	8.03 ± 1.69^{g}	20.26 ± 1.73^{e}	2.50	120.76 ± 10.09^{l}	0.58 ± 0.05^{d}
Group (11)	15.8 ± 1.08^{g}	29.6 ± 1.46^{g}	1.87	211.20 ± 10.06^{l}	0.88 ± 0.07^{d}
LSD 5%	4.322	2.037		4.854	0.230

Each value represents the mean of 5 rats (Mean ± SD). The same letters in each column represent the insignificant difference at $P<0.05$. Group (1): control; group (2): PPE (1 mg); group (3): PPE (5 mg); group (4): $NaBH_4$-AgNPs (1 mg); group (5): $NaBH_4$-AgNPs (5 mg); group (6): PPE-AgNPs (1 mg); group (7): PPE-AgNPs (5 mg); group (8): ST-AgNPs (1 mg); group (9): ST-AgNPs (5 mg); group (10): PPE/ST-AgNPs (1 mg) and group (11): PPE/ST-AgNPs (5 mg).

3.7.2. Protein profile of the experimental animals

As illustrated in Table (9), the action of synthesized AgNPs on the values of total soluble proteins, albumin, globulin and the ratio of albumin/globulin was evaluated. The results revealed non-significant changes observed in the level of globulin and albumin/globulin ratio, but a significant increase in total proteins and albumin levels with PPE (1 mg) administration as compared to the normal control group. The administration of PPE (5 mg) showed significant increase in the levels of total proteins, albumin, and globulin but non-significant changes were observed in albumin/globulin ratio (A/G) as compared to the normal control. Animals administered with $NaBH_4$-AgNPs (1 mg) showed significant changes in total proteins, albumin and globulin and a significantly decreased albumin/globulin ratio as compared to the normal control group. Administration of $NaBH_4$-AgNPs (5 mg) significantly also decreased the levels of total proteins, albumin, globulin and albumin/globulin ratio as compared to the normal control, but more than low level (1 mg). As for PPE-AgNPs (1 mg) group, a non-significant change in the levels of total proteins, albumin, and globulin was illustrated, but a significant increase in the albumin/globulin ratio was shown as compared to the normal control. Administered of PPE-AgNPs (5 mg) exhibited a significant reduction in the globulin level and significantly decreased the albumin/globulin ratio, but non-significant changes in the levels of total proteins and albumin were observed as compared to normal control group. A significant increase was observed in level of globulin, but a significant reduction in the albumin/and globulin ratio and non-significant changes in total proteins and albumin levels when ST-AgNPs (1 mg) was compared to the normal control. ST-AgNPs (5 mg), PEE/ST-AgNPs (1 mg and 5 mg) groups revealed a significant increase in total proteins, albumin, and globulin levels but significant reduction in the ratio of albumin/globulin as compared to the normal control group.

Alterations in the percentages of serum proteins following treatment with PPE, $NaBH_4$-AgNPs, PPE-AgNPs, ST-AgNPs, and PPE/ST-AgNPs indicate formulation- and dose-dependent alterations in protein synthesis in the liver and protein metabolism in the system. Low-dose PPE (1 mg) was significantly correlated with total protein and albumin but not with globulin or A/G ratio, whereas the 5 mg dose maximally elevated all three parameters but did not alter the A/G ratio, suggesting that PPE per se acts to enhance hepatic synthetic activity most significantly without causing significant protein distribution alteration. In contrast, $NaBH_4$-AgNPs caused broader dysregulation, with the 1 mg dose lowering the A/G ratio in the face of protein fraction increases and the 5 mg dose causing general reductions across total proteins, albumin, and globulin, as seen with reported nanoparticle-induced hepatocellular injury and impaired protein synthesis **[62,67]**. The PPE-AgNPs had a more nuanced profile: the 1 mg dose caused few alterations apart from increasing the A/G ratio, while 5 mg decreased globulin and A/G ratio without noticeably altering total protein or albumin. ST-AgNPs and PPE/ST-AgNPs at both doses increased total proteins, albumin, and globulin but decreased the A/G ratio, a pattern that can suggest disproportionate globulin

overproduction or altered albumin turnover. Such alteration of protein fractions has been associated with inflammatory response, oxidative stress, and suppression of hepatic biosynthetic activity in AgNP-treated models **[62,67]**. This indicates that, while plant extract per se can activate protein synthesis, its nanoparticle formulations particularly at high doses can have multifaceted metabolic or immunomodulatory effects that require further histopathological and mechanistic evidence.

Table 9: Protein profile of the experimental animals

Treatment	Total protein (g/dL)	Albumin (g/dL)	Globulin (g/dL)	A/G Ratio
Group (1)	6.62±0.68^{a}	4.09±0.81^{a}	2.53	1.61
Group (2)	7.14±0.64^{ab}	4.54±0.21^{ab}	2.60	1.74
Group (3)	7.70±0.12^{ab}	4.82±0.15^{ab}	2.88	1.67
Group (4)	6.82±0.62^{ab}	3.45±0.35^{ab}	3.37	1.02
Group (5)	4.98±0.44^{ab}	2.65±0.25^{ab}	2.33	1.13
Group (6)	6.90±0.14^{ab}	4.64±0.29^{bc}	2.26	2.05
Group (7)	6.68±0.67^{ab}	5.34±0.18^{bc}	1.34	3.98
Group (8)	7.00±0.67^{ab}	3.61±0.37^{bc}	3.40	1.06
Group (9)	7.18±0.09^{b}	3.32±0.38^{cd}	3.86	0.86
Group (10)	7.20±0.76^{b}	4.18±0.15^{cd}	3.02	1.38
Group (11)	7.46±0.74^{c}	4.46±0.28^{d}	3.00	1.48
LSD 5%	0.585	0.756	0.954	

Each value represent the mean of 5 rats (Mean ± SD). The same letters in each column represents the insignificant difference at P<0.05. Group (1): control; group (2): PPE (1 mg); group (3): PPE (5 mg); group (4): $NaBH_4$-AgNPs (1 mg); group (5): $NaBH_4$-AgNPs (5 mg); group (6): PPE-AgNPs (1 mg); group (7): PPE-AgNPs (5 mg); group (8): ST-AgNPs (1 mg); group (9): ST-AgNPs (5 mg); group (10): PPE/ST-AgNPs (1 mg) and group (11): PPE/ST-AgNPs (5 mg).

3.7.3. Kidney function of experimental animals

The synthesized AgNPs effects on the levels of urea, uric acid and creatinine were determined (Table 10). The results showed a significant decrease observed in urea levels and a significant increase in uric acid and creatinine levels with PPE (1 mg) administration as compared to the normal control group. The administration of PPE (5 mg) showed a significant increase in the levels of uric acid and a significant decrease in urea levelsbut non-significant changes were observed in creatinine as compared to the normal control. In administrated animals with $NaBH_4$-AgNPs (1 mg), there were slightiy significant changrs in urea and creatinine levels, but significantly increased the level of uric acid as compared to the normal control group. Administration of $NaBH_4$-AgNPs (5 mg) significantly increased the levels of urea, uric acid and creatinine as compared to the normal control. As for PPE-AgNPs (1 mg) group, non-significant changes in the levels of uric acid, a significant increase in the creatinine levels and a significant decrease in the levels of urea were shown as compared to the normal control. Administration of PPE -AgNPs (5 mg) exhibited a significant reduction in the creatinine level and significantly increased the urea and uric acid as compared to the normal control group. A significant increase was observed in levels of uric acid and creatinine, but a non-significant change in urea levels when ST-AgNPs (1 mg) were compared to the normal control. ST-AgNPs (5 mg) group revealed a significant increase in urea, uric acid and creatinine levels as compared to the normal control group. The results demonstrated that PPE/ST-AgNPs (1 mg) had a significant increase in the levels of uric acid and creatinine, and a significant decrease in the urea, but PPE/ST-AgNPs (5 mg) significantly increased the urea and uric acid levels, but did not significantly affect the levels of creatinine.

Table 10: Kidneys function of the experimental animals

Treatment	Urea (mg/dL)	Uric acid (mg/dL)	Creatinine (mg/dL)
Group (1)	32.16±1.65^{a}	2.70±0.18^{a}	0.84±0.04^{a}
Group (2)	25.63±1.02^{b}	3.10±0.26^{b}	1.07±0.04^{b}
Group (3)	20.02±1.47^{c}	3.10±0.32^{bc}	0.85±0.02^{b}
Group (4)	33.52±1.77^{D}	4.79±0.28^{bc}	0.90±0.08^{b}
Group (5)	54.74±1.94^{e}	8.24±0.73^{bc}	1.71±0.11^{b}
Group (6)	27.58±1.72^{e}	2.83±0.23^{cd}	1.09±0.12^{b}
Group (7)	40.64±1.71^{f}	4.61±0.42^{cd}	0.79±0.08^{b}
Group (8)	32.0±1.80^{fg}	3.50±0.22^{cd}	1.16±0.06^{b}
Group (9)	44.12±3.12^{gh}	5.46±0.41^{d}	1.90±0.07^{c}
Group (10)	29.38±1.61^{h}	3.97±0.36^{d}	1.04±0.06^{c}
Group (11)	37.46±2.15^{T}	4.02±0.35^{d}	0.88±0.06^{c}
LSD 5%	2.720	0.947	0.240

Each value represents the mean of 5 rats (Mean ± SD).The same letters in each column represent the insignificant difference at P<0.05. Group (1): control; group (2): PPE (1 mg); group (3): PPE (5 mg); group (4): $NaBH_4$-AgNPs (1 mg); group (5): $NaBH_4$-AgNPs (5 mg); group (6): PPE-AgNPs (1 mg); group (7): PPE-AgNPs (5 mg); group (8): ST-AgNPs (1 mg); group (9): ST-AgNPs (5 mg); group (10): PPE/ST-AgNPs (1 mg) and group (11): PPE/ST-AgNPs (5 mg).

3.7.4. Lipid profile of the experimental animals

As shown in Table (11), the action of synthesized AgNPs on the levels of triglycerides, cholesterol, HDL-c, LDL-c and vLDL-c addition to the risk ratio of cholesterol/HDL and LDL/HDL, was evaluated. The results revealed that a significant decrease was observed in levels of triglycerides with the PPE (1 mg) administration but recorded a significant increase was recoeded the administration of other treatments, as compared to the normal control group. The administration of PPE (1mg and 5 mg) showed a significant decrease in the levels of cholesterol, but non-significant changes were observed with the administered PEE/ST-AgNPs (1 mg) as compared to the normal control. The other treatments significantly increased the cholesterol levels. Administration with PPE (1mg), PPE-AgNPs (1 mg) and ST-AgNPs (1 mg) were non-significantly changed the level of HDL-c but administration of $NaBH_4$-AgNPs (1 mg and 5 mg), PPE-AgNPs (5 mg) and ST-AgNPs (5 mg) significantly decreased the level of HDL-c and the other treatments had a significant increase as compared to the normal control group. Administration of PPE (1 mg and 5 mg) and PEE/ST-AgNPs (5 mg) significantly decreased the level of LDL-c but PEE/ST-AgNPs (1 mg) recorded non-significant changes, and the other treatments showed a significant increase as compared to the normal control. As illustrated, a significant decrease in the level of vLDL-c was evaluated when the animals were adminiditere with PPE (5 mg), but PEE/ST-AgNPs (1 mg) revealed non-significant changes, and the other treatments significantly increased the vLDL-c levels as compared to the normal control. Administration of PPE (5 mg) and PEE/ST-AgNPs (5 mg) significantly decreased the risk ratio of cholesterol/HDL and LDL/HDL, but PPE (1 mg) and PEE/ST-AgNPs (1 mg) recorded non-significant changes, and the other treatments showed a significant increase as compared to the normal control.

The alteration of the serum lipid parameters by treatment with PPE, $NaBH_4$-AgNPs, PPE-AgNPs, ST-AgNPs, and PPE/ST-AgNPs suggests that plant extract and its nanoparticle preparations exert differential effect on lipid metabolism as well as cardiovascular risk factors. Low-dose PPE (1 mg) reduced triglycerides and cholesterol but not HDL-c and LDL-c, reflecting a putative hypolipidemic activity as reported in findings of polyphenolic compounds with better lipid clearance and de novo lipogenesis inhibition [62]. High-dose PPE (5 mg) also reduced LDL-c, vLDL-c, and risk ratios (cholesterol/HDL and LDL/HDL), further reflecting its putative cardioprotective activity. On the other hand, $NaBH_4$-AgNPs at both doses significantly elevated cholesterol, triglycerides, LDL-c, and vLDL-c but reduced HDL-c, indicating widespread dyslipidemia most probably induced by AgNP-triggered oxidative stress, hepatocellular damage, and dyslipidemia transport mechanisms **[67]**. Both ST-AgNPs and PPE-AgNPs showed dose-dependent activities in which the 1 mg dose did not cause significant lipid disturbances, but the 5 mg dose decreased HDL-c and atherogenic lipids and risk ratios, indicating nanoparticle-induced metabolic toxicity. Surprisingly, 5 mg of PPE/ST-AgNPs mimicked the therapeutic lipid-lowering efficacy of PPE alone, whereas 1 mg was less effective, which implies co-functionalization of nanoparticles could preserve partially the bioactivity of PPE at the higher concentration. The findings are in agreement with the fact that the physicochemical properties of nanoparticles including size, surface chemistry, and bio-distribution strongly influence their metabolic interactions and safety profile **[67]**. Collectively, the evidence highlights that while PPE in itself is hypolipidemic, its nanoparticle formulations, in a technique- and dose-dependent approach, could either suppress or enhance dyslipidemia, calling for detailed mechanistic exploration to maximize their therapeutic index.

Table 11: Lipid profile of the experimental animals

Treatment	Triglycerides (mg/dL)	Cholesterol (mg/dL)	HDL-c (mg/dL)	LDL-c (mg/dL)	vLDL-c (mg/dL)	Risk ratio ($\frac{total\ cholesterol}{HDL}$)	Risk ratio (
Group (1)	91.00±8.97	127.56±11.33^{a}	41.34±2.69^{a}	68.66±4.11	18.20±1.39	3.09	1.66
Group (2)	107.52±6.20	117.86±11.38^{b}	39.86±1.84^{a}	56.40±4.00	21.50±2.24	2.96	1.41
Group (3)	75.69±6.99	105.08±10.29^{c}	57.86±3.93^{b}	31.80±3.00	15.41±1.38	1.82	0.55
Group (4)	116.40±10.95	147.52±11.08^{c}	33.44±1.10^{c}	91.80±8.00	23.28±2.97	4.41	2.75
Group (5)	209.66±13.41	246.48±21.65^{c}	22.90±1.93^{c}	181.00±16.00	41.93±3.71	10.76	7.90
Group (6)	116.86±9.70	149.72±11.31^{c}	39.68±3.17^{c}	86.60±7.12	23.37±1.74	3.77	2.18
Group (7)	132.22±12.57	149.00±14.12^{d}	33.44±1.92^{c}	89.60±8.10	26.44±2.51	4.46	2.68
Group (8)	137.30±11.95	150.96±12.25^{e}	41.24±2.97^{c}	82.60±7.21	27.46±2.39	3.66	2.00
Group (9)	134.34±13.42	162.22±13.17^{e}	34.94±2.69^{c}	100.20±10.00	26.87±2.86	4.64	2.87
Group (10)	103.86±9.67	131.47±11.97^{f}	48.78±3.14^{c}	62.20±6.12	20.77±2.93	2.70	1.28
Group (11)	125.70±11.90	138.47±12.38^{g}	56.00±4.83^{d}	57.80±5.12	25.14±2.39	2.47	1.03
LSD 5%	3.400	6.241	5.378	2.700			

Each value represents the mean of 5 rats (Mean ± SD). The same letters in each column represents the insignificant difference at P<0.05. Group (1): control; group (2): PPE (1 mg); group (3): PPE (5 mg); group (4): $NaBH_4$-AgNPs (1 mg); group (5): $NaBH_4$-AgNPs (5 mg); group (6): PPE-AgNPs (1 mg); group (7): PPE-AgNPs (5 mg); group (8): ST-AgNPs (1 mg); group (9): ST-AgNPs (5 mg); group (10): PPE/ST-AgNPs (1 mg) and group (11): PPE/ST-AgNPs (5 mg).

3.7.5. Complete Blood Capture(CBC) of the experimental animals

The total number of Wight blood cells (WBCs), red blood cells (RBCs), hemoglobin (Hb) content, hematocrit (Hct) percent and the number of platelets (Plt) were illustrated in Table (12). The results showed that the total number of WBC values significantly increased in the groups that was injected with $NaBH_4$-AgNPs (5 mg) and ST-AgNPs (1 mg and 5 mg), but in the other groups, the total number of WBC values were significantly unchanged in comparison with the control group. The total count of RBCs showed a significant increase in the group of animals that were treated with PPE (5 mg) and a significant

decrease in the group of animal that were treated with $NaBH_4$-AgNPs (5 mg) but did not change in the groups of animals that were treated with other treatmentsin comparison with the control group.The number of Plt was significantly increased after treatment of animals with PPE/ST-AgNPs (1 mg) and significantly decreased in the group that was treated with PPE (1 mg), $NaBH_4$-AgNPs (5 mg), ST-AgNPs (1 mg and 5 mg), but did not change significantly in the groups of animals that were treated with other treatments in comparison with the control group.A significant decrease in Hb content was observed in the group injected with $NaBH_4$-AgNPs (5 mg), and in Hb content was significantly increased after injection with PPE (1 mg and 5 mg) and PPE/ST-AgNPs (5 mg), but non-significant changes were observed in the other groups in comparison with the control group. The Hct percent was significantly decreased and observed in the group treated with $NaBH_4$-AgNPs (5 mg), and also was significantly increased after administering PPE (1 mg and 5 mg) and PPE/ST-AgNPs (5 mg), but non-significant changes were observed in the other groups in comparison with the control group.

These results showed variant alterations in blood picture and number of RBC parameters that might illustrate how AgNPs affect hemoglobin synthesis as red blood cells mature during bone marrow formation **[68]**. WBCs play a crucial part in the body's immune response; they are the first line of defense. Various kinds of neutrophils can signal an infection, an allergic reaction, or a toxic reaction to medications or toxins. Hypoxia causes anemia, and the decrease in RBC count reveals that there was more breakdown of RBC .This deficiency could be attributed to an inadequate supply of iron, cobalamin, or folic acid, or it could be owing to chronic diseases or toxic substances that negatively affect the RBCs count produced by the bone marrow. AgNPs administered orally and intraperitoneally have a toxic impact on RBCs **[69]**.

AgNPs cause disturbances in the function of the immune system. Likely, the reduction of the circulating hormone and erythropoietin—a glycoprotein that promotes erythropoiesis—caused a slight dip in RBCs and Hb **[70].** Erythropoietin deficiency (depletion in blood concentration of erythropoietin) can cause normochromic, normocytic anemia **[71]**. Hypochromic anemia is a generic term for any type of anemia, even though iron deficiency is by far the most prevalent cause**.** Because Plt plays a crucial role in blood coagulation, an increase in Plt counts causes a thrombus to form inside blood arteries, which accelerates the development of atherosclerosis brought by AgNP administration. AgNPs may cause cell toxicity by attaching to sulfur and phosphorus-containing biomolecules, such as DNA or other biological components. The cytotoxicity of AgNPs has been demonstrated in relation to the production of free radicals, which distorts cell membranes **[72]**. Furthermore, AgNPs exhibit toxicological characteristics and cause inadequate metabolic activity **[73]**. The biokinetics of AgNPs cytotoxicity effect is influenced by their chemical structure, shape, size, agglomeration, surface, and function **[74]**. As a result, AgNPs have a toxic effect given that they directly interact with RBCs, eliciting oxidative stress, membrane damage, and hemolysis. Nevertheless, taxological data affect RBCs in different ways, and the processes underlying these effects are still poorly understood **[75]**.

AgNPs cause lipid peroxidation and hemolysis due to membrane damage, along with a fair amount of antioxidant enzyme synthesis. Also, hemolysis and membrane damage can be induced by small-sized AgNPs. As a result of the interaction between erythrocytes and AgNPs, the size and concentration of AgNPs are predisposing factors that impact RBCs.In general, AgNPs administration in rats caused decreases in the level of Hb, RBC and Hct but increases in the level of Plt and WBC. It means that AgNPs have a harmful effect on blood animals. In the blood, **Jeong *et al.* [76]** showed that the silver from the nanoparticles that are ingested orally can reach other organs through the bloodstream. These effects may be caused by particles rather than ionized silver because comparable effects have not been previously documented for soluble silver.

Table 12: Complete Blood Capture (CBC) of the experimental animals

Treatment	WBCs ($x10^9$/L)	Hb (g/d)	RBCs ($x10^{12}$/L)	Hct (%)	Plt ($x10^{10}$/L)
Group (1)	4.85 ± 0.32^{c}	13.97 ± 1.1^{b}	5.54 ± 0.46^{b}	39.12 ± 5.5^{d}	757 ± 76^{b}
Group (2)	5.55 ± 0.42^{c}	13.27 ± 1.2^{a}	5.25 ± 0.52^{b}	45.55 ± 4.1^{b}	788 ± 72^{c}
Group (3)	5.67 ± 0.51^{c}	15.82 ± 0.8^{a}	6.73 ± 0.65^{a}	47.42 ± 3.5^{a}	835 ± 81^{bc}
Group (4)	5.22 ± 0.50^{c}	13.25 ± 1.4^{b}	4.79 ± 0.44^{b}	39.70 ± 2.2	816 ± 76^{b}
Group (5)	13.95 ± 0.20^{a}	10.30 ± 1.0^{c}	3.44 ± 0.34^{c}	40.90 ± 2.4	898 ± 55^{d}
Group (6)	4.85 ± 0.26^{c}	14.10 ± 1.3^{b}	5.12 ± 0.50^{b}	42.47 ± 4.7^{c}	861 ± 75^{b}
Group (7)	5.55 ± 0.53^{c}	14.02 ± 1.6^{b}	5.18 ± 0.49^{b}	41.85 ± 4.3^{c}	669 ± 52^{c}
Group (8)	7.75 ± 0.40^{b}	13.80 ± 1.1^{b}	4.87 ± 0.38^{b}	42.47 ± 4.2^{c}	727 ± 61^{c}
Group (9)	6.95 ± 0.46^{b}	14.50 ± 1.3^{b}	5.19 ± 0.52^{b}	42.50 ± 3.1^{c}	735 ± 72^{c}
Group (10)	5.65 ± 0.34^{c}	14.10 ± 1.3^{b}	4.89 ± 0.38^{b}	41.40 ± 3.5^{c}	916 ± 86^{a}
Group (11)	4.82 ± 0.30^{c}	15.70 ± 1.2^{a}	4.94 ± 0.45^{b}	44.47 ± 4.2^{bc}	887 ± 85^{b}

Each value represents the mean of 5 rats (Mean ± SD). The same letters in each column represent the insignificant difference at $P<0.05$. Group (1): control; group (2): PPE (1 mg); group (3): PPE (5 mg); group (4): $NaBH_4$-AgNPs (1 mg); group (5): $NaBH_4$-AgNPs (5 mg); group (6): PPE-AgNPs (1 mg); group (7): PPE-AgNPs (5 mg); group (8): ST-AgNPs (1 mg); group (9): ST-AgNPs (5 mg); group (10): PPE/ST-AgNPs (1 mg) and group (11): PPE/ST-AgNPs (5 mg).

3.7.6. Fasting blood glucose (FBG) level

The FBG level in Table (13) showed a significant decrease in the group of animals that were administered with PPE-AgNPs (5 mg)and did not show any significant changes in the groups of animals that were treated with PPE (1 mg) and PPE-AgNPs (1 mg), but significant changes dose with increasing were observed in the other groups when compared to the control group.AgNPs have the potential to cause insulin sensitivity because they raise the concentration of calcium ions in the cytosol

and phosphorylate AMPK via the CAMKKβ pathway in rats and SH-SY5Y cells. AMPK activation increases insulin sensitivity and may mediate the action of insulin by enhancing its activity **[77]**. When insulin binds to its receptor, it initiates the phosphorylation cascade from IRS1, which results in the transport of glucose into the cells.AgNPs raise the expression levels of IRS1 and GLUT2, which lowers blood glucose levels. Additionally, AgNPs increase the levels of insulin expression and secretion **[78]**.

Table 13: Blood glucose of the experimental animals

Treatment	Blood glucose (mg/dl)
Group (1)	73.96 ± 4.72^{f}
Group (2)	71.48 ± 5.66^{g}
Group (3)	90.62 ± 4.15^{d}
Group (4)	87.82 ± 4.31^{d}
Group (5)	186.46 ± 10.79^{a}
Group (6)	76.78 ± 6.46^{f}
Group (7)	59.58 ± 4.74^{h}
Group (8)	83.66 ± 6.75^{e}
Group (9)	107.24 ± 4.79^{b}
Group (10)	95.56 ± 8.33^{c}
Group (11)	103.1 ± 7.62^{b}

Each value represents the mean of 5 rats (Mean ± SD). The same letters in each column represent the insignificant difference at $P<0.05$. Group (1): control; group (2): PPE (1 mg); group (3): PPE (5 mg); group (4): $NaBH_4$-AgNPs (1 mg); group (5): $NaBH_4$-AgNPs (5 mg); group (6): PPE-AgNPs (1 mg); group (7): PPE-AgNPs (5 mg); group (8): ST-AgNPs (1 mg); group (9): ST-AgNPs (5 mg); group (10): PPE/ST-AgNPs (1 mg) and group (11): PPE/ST-AgNPs (5 mg).

3.8. Genotoxicity investigation of liver cell

AgNPs could significantly change the expression of the Bax and Bcl-2 genes, as shown in Table (14). The findings demonstrated that cells exposed to PPE (5 mg) and $NaBH_4$-AgNPs (1 mg) had an overexpression of the pro-apoptotic gene Bax compared to the control. The expression of antiapoptotic gene Bcl-2 was remarkably down-regulated in $NaBH_4$-AgNPs (1 mg and 5 mg), PPE-AgNPs (1 mg) and PPE/ST-AgNPs (1 mg and 5 mg), and up-regulated in PPE (1 mg and 5 mg), PPE-AgNPs (5 mg) and ST-AgNPs (5 mg) compared with the control. A noticeable significant increase in CASP-3 activity was observed when the cells were exposed to PPE (5 mg), $NaBH_4$-AgNPs (1 mg), PPE-AgNPs (5 mg), ST-AgNPs (1 mg and 5 mg) and PPE/ST-AgNPs (5 mg) compared to the control cells. The activity level was significantly lower in PPE (1 mg), $NaBH_4$-AgNPs (5 mg), PPE-AgNPs (1 mg) and PPE/ST-AgNPs (1 mg) compared to the control.BAX is a pro-apoptotic protein that promotes cell death. Meanwhile, BCL-2 is an anti-apoptotic protein that inhibits cell death.CASP-3 is a key executioner caspase involved in the apoptotic process. So BAX, BCL-2 and CASP-3 are key players in apoptosis. AgNPs have a role in regulating apoptosis via interacting with cells in various ways, including direct cellular uptake which AgNPs can be internalized by cells, leading to intracellular interactions, or AgNPs have the ability to produce reactive oxygen species (ROS), which can destroy cellular components and cause oxidative stress, also AgNPs can trigger inflammatory responses, which may contribute to cell death. The effect of AgNPs on BAX, BCL-2, and CASP-3 can vary depending on several factors: (1) Different sizes and shapes of AgNPs can exhibit varying toxicity and cellular interactions. (2) Higher concentrations of AgNPs may lead to more significant effects on apoptosis. (3) The sensitivity of cells to AgNPs can vary depending on their type and physiological state. These results showed that AgNPs can increase Bax expression, which can promote apoptosis by activating the intrinsic apoptotic pathway, decrease BCL-2 expression, which can further promote apoptosis by reducing the inhibition of cell death and activate CASP-3, which can initiate the execution phase of apoptosis, leading to cell, death .Changes in the expression of apoptotic-related genes may have caused apoptosis. Therefore, the expression of the BAX and BCL-2 genes, which efficiently support the apoptotic pathway, was investigated. Regarding the apoptotic effects of AgNPs, certain studies have demonstrated their encouraging anticancer potential, which results in an up-regulation of Bax and a decrease in the expression of the Bcl-2 gene **[79, 80]**. Overexpression of BAK and BAX, two members of the BCL-2 family, has been shown to sensitize cells to apoptosis by causing the outer mitochondrial membrane to permeabilize, which releases proteins into the cytosol. Cell death is then triggered by the activation of caspase enzymes **[81]**. **Soni and Gandhi [82]** illustrated that concern over the harmful effects of silver nanoparticles (AgNPs) on living things and the environment has grown as their use expands. Human blood and promyelocytic leukemic (HL-60) cells were used as an *in vitro* model to study the cytotoxicity and genotoxicity of AgNPs made with the plant flavonoid Naringin as a reducing agent. The activation of caspase suggests that AgNPs can interact with DNA and cause cell death. DNA fragmentation, a sign of apoptosis, was examined for further validation. AgNPs caused a DNA laddering pattern as their concentration increased. This suggests that AgNPs have the ability to be genotoxic to cells.

Table 14: BAX, CASP-3 and BCL-2 activities in liver tissue homogenate

	BAX ng/g tissue	CASP-3 ng/g tissue	BCL-2 ng/g tissue
Group 1	953.52	327.76	50.40
Group 2	831.46	178.11	75.12
Group 3	2199.8	501.94	99.47
Group 4	1266.54	694.24	38.78
Group 5	441.67	155.39	35.53
Group 6	205.80	13.04	28.51
Group 7	973.37	539.59	66.43
Group 8	695.45	1141.44	52.14
Group 9	951.14	3908.22	91.48
Group 10	298.00	278.23	20.16
Group 11	626.09	462.45	26.69

Group (1): control; group (2): PPE (1 mg); group (3): PPE (5 mg); group (4): $NaBH_4$-AgNPs (1 mg); group (5): $NaBH_4$-AgNPs (5 mg); group (6): PPE-AgNPs (1 mg); group (7): PPE-AgNPs (5 mg); group (8): ST-AgNPs (1 mg); group (9): ST-AgNPs (5 mg); group (10): PPE/ST-AgNPs (1 mg) and group (11): PPE/ST-AgNPs (5 mg).

3.9. Histopathological examination

Following the necessary treatment, the testes, liver, and kidneys were removed from each group for histological examination. Overall, the histological analysis demonstrated that high dosages of AgNPs more fully repaired the necrotic and injured tissues.

3.9.1. Histopathological examination of Liver samples

The portal vein and portal triad are shown in liver slices in all groups stained with H&E at 400X magnification (Figure 10). Group (1) displayed a normal liver structure, with sinusoids separating the hepatic cords that radiate from the major vein. Group (2) showed mild vacuolar degeneration of hepatic cells with mild activation of kupffer cells. Group (3) showed distortion and disorganization of the hepatocytes, mild dilatation of hepatic sinusoids with mild activation of kupffer cells and fibroblast infiltration was noticed (arrow). Group (4) showed dilatation, congestion of the portal blood vessels, and edema of the portal triad which was tinged with mononuclear inflammatory cell infiltration in addition to newly formed bile ductules (arrow). Group (5) showed congestion of the portal blood vessels associated with mononuclear severe inflammatory cell infiltration and newly formed bile ductules, individual alteration of hepatocytes, some hepatic cells appeared necrotic with karyolysis of the nuclei, others revealed mild pleomorphic nuclei. Group (6) showed mild dilatation of hepatic sinusoids with mild mononuclear inflammatory cells infiltration in addition to hepatic cells disarrangement and distortion, also sporadic hepatocellular necrosis was present. Group (7) showed mild dilatation of hepatic sinusoids with mild mononuclear inflammatory cells infiltration in addition to distortion and disorganization with individualization of the hepatocytes, mild pleomorphic nuclei, and individual alteration of hepatocytes. Group (8) showed mild dilatation of hepatic sinusoids with mild mononuclear inflammatory cell infiltration in addition to hepatic cell disarrangement and sporadic hepatic cell necrosis. Group (9) showed dilatation and congestion of hepatic blood vessels with severe sinusoidal leukocytosis (appearance of mononuclear cells in the dilated hepatic sinusoids), distortion and disorganization of the hepatocytes in addition to mild pleomorphic nuclei. Group (10) showed dilatation of hepatic blood vessels, mild activation of kupffer cells, in addition to hepatocellular coagulative necrosis, some hepatic cells showing vacuolation in nuclei (arrow). Group (11) showed mild dilatation and congestion of the hepatic sinusoids with mononuclear inflammatory cell infiltration (arrow), some hepatic cells appeared necrotic in addition to distortion and disorganization of the hepatocytes with mild pleomorphism.

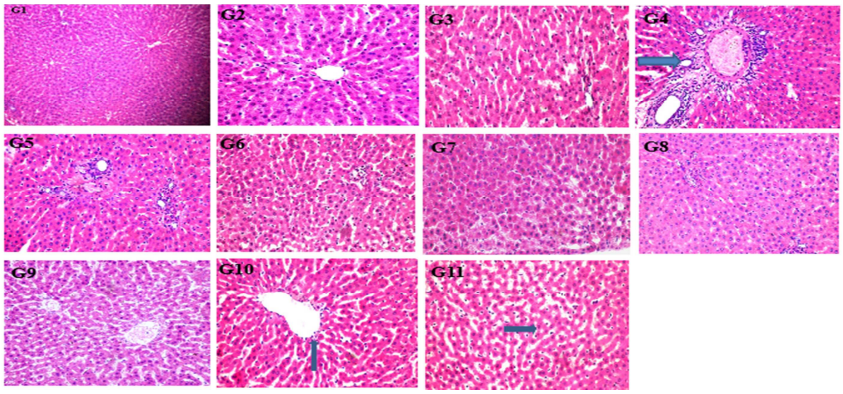

Figure 10: Histological examination liver from rat groups.

3.9.2. Histopathological examination of kidney samples

Kidney slices stained with H&E from each group were examined, with particular attention paid to the arrangement and border of the glomerulus and renal tubules at 400X magnification (Figure 11). Group (1) showed normal glomerular and renal tubular. In group (2) ,some renal tubules in the medulla showed mild vacuolar degeneration of the epithelium lining with the renal cast formation in their lumen. In group (3), some renal tubules revealed mild cystic dilatation (arrow) others showed coagulative necrosis with pyknotic nuclei. Group (4) showed subcapsular hemorrhage (arrow), and necrobiotic changes of epithelium lining renal tubules. Group (5) showed perivascular edema (star), necrobiotic severe changes in the epithelium lining renal tubules, atrophy and shrinkage of some glomeruli were detected (arrow), and some others illustrating hypertrophy of glomerular tuft capillary with the absence of glomerular Bowman,s. Group (6) showed mild perivascular edema, interstitial edema (star) ,necrobiotic changes in epithelium lining renal tubules, in addition to some renal glomeruli illustrating hypertrophy of glomerular tuft capillaries with the absence of glomerular Bowman,s space (arrow). Group (7) showed mild perivascular edema (star), and coagulative necrosis of the epithelium lining renal tubules with pyknotic nuclei. Group (8) showed perivascular edema (star), mild coagulative necrosis of epithelium lining renal tubules with pyknotic nuclei and renal cast formation in their lumen (blue arrow). Group (9) showed perivascular edema (star), some renal tubules revealed necrobiotic changes of the epithelium lining with the renal cast formation in their lumen, others showing cystic dilatation (yellow arrow) in addition to hypercellularity of glomerular tuft capillaries with absence of Bowman,s space (blue arrow). Group (10) showed mild necrobiotic changes of the epithelium lining renal tubules and some glomeruli showing hypertrophy of glomerular tuft capillaries with narrowing of Bowman,s space (blue arrow). In group (11), the renal medulla showed vacuolar degeneration in the epithelium lining renal tubules with renal cast formation in their lumen (arrow).

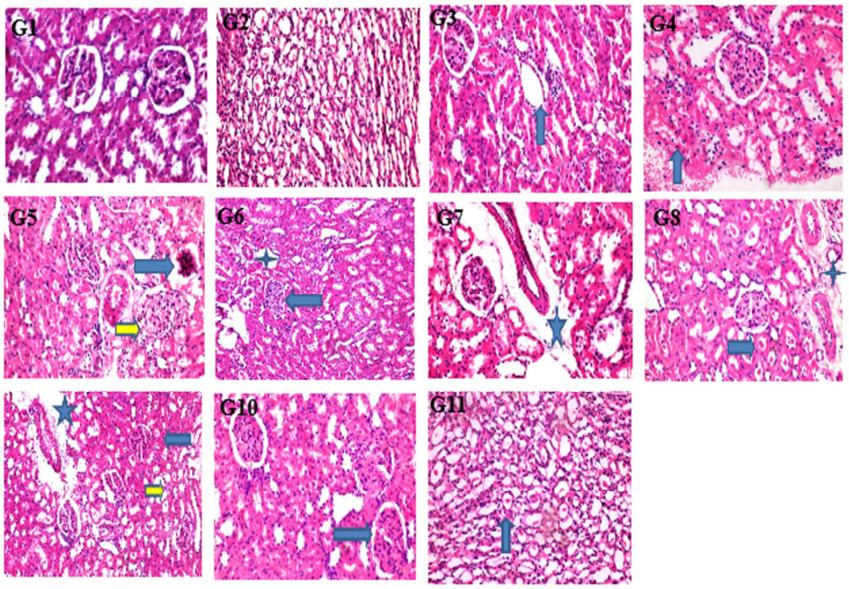

Figure 11: Histological examination of the kidney from rat groups.

3.9.3. Histopathological examination of testes samples

In order to compare the morphology of each group, tests from each group were H&E stained, and histological analysis was performed at different magnifications. Seminiferous tubules and normal spermatogenic cells were focused on 400X in all groups (Figure 12). Group (1) showed normal histological structure of seminiferous tubules with normal spermatogenic cells. In group (2), some seminiferous tubules showed necrobiotic changes with marked depletion in germ cells. Group (3) revealed irregular contouring Of seminiferous tubules (arrow) and interstitial edema (star). In group (4), simple cystic transformation of rete testis lining by squamous epithelium cells showed depletion and vacuolation. Group (5) showed interstitial edema (star), irregular contouring of the basal lamina of seminiferous tubules, severe necrobiotic changes and loss of normal orientation of the germ cells (arrow). In group (6), some seminiferous tubules revealed degeneration and necrosis of spermatogenic cells with vacuolation of Sertoli cells. In group (7), some seminiferous tubules showed sloughing of spermatogenic cells in the lumen (red arrow), necrobiotic changes and loss of normal orientation of the germ cells in addition to the appearance of vacuoles in the spermatogenic epithelium in some seminiferous tubules (arrow). Group (8) showed a reduction in the number of germ cells with the appearance of large spaces or vacuoles in the spermatogenic epithelium (arrow). Group (9) showed interstitial edema (star), irregular contouring of basal lamina of seminiferous tubules, and necrobiotic changes of the germ cells. In group (10), some seminiferous tubules showed normal structure others revealed necrobiotic changes with depletion and loss of the normal orientation of the germ cells. Group (11) showed mild necrobiotic changes and loss of the normal orientation of the germ cells in addition to vacuoles in the spermatogenic epithelium in some seminiferous tubules (arrow).

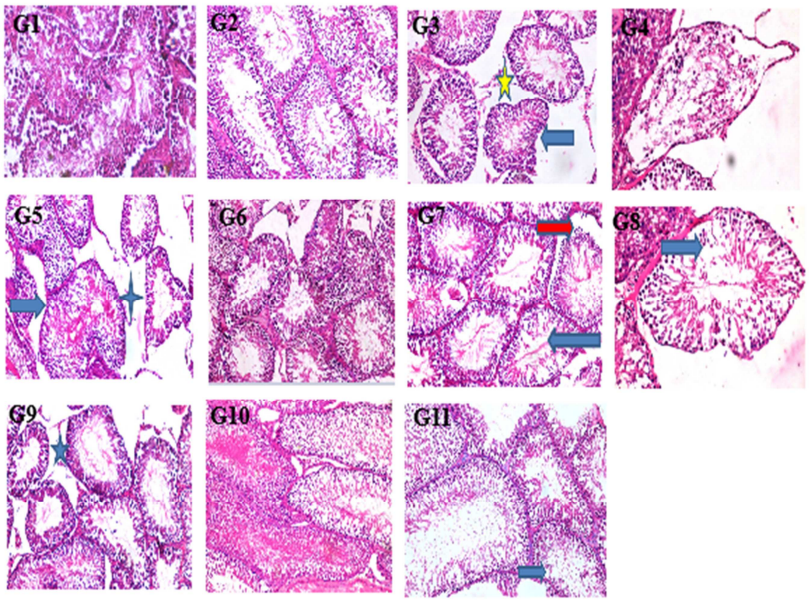

Figure 12: Histological examination of testes from rat groups.

Histopathological analysis showed dose- and formulation-dependent testis, kidney, and liver alterations following exposure to the plant extract, silver nanoparticles (AgNPs), and their combination formula. The control group alone had ordered hepatic cords and sinusoids architecture, and rats exposed to PPE had mild vacuolar degeneration with Kupffer cell activation (Figure 10). $NaBH_4$-AgNPs and some PPE/ST-AgNP groups induced more serious lesions like sinusoidal dilatation, mononuclear inflammatory infiltration, recruitment of fibroblasts, portal congestion, bile duct proliferation, scattered to coagulative hepatocellular necrosis, suggestive of progressive hepatocellular damage characteristic of AgNP-induced oxidative stress and inflammation [62,67]. Kidney sections (Figure 11) also showed parallel changes, ranging from faint vacuolation of the tubules and formation of renal casts in low-dose PPE groups to massive necrobiotic alteration, glomerular atrophy or hypertrophy, perivascular/interstitial edema, and disappearance of Bowman's space in $NaBH_4$-AgNPs and high-dose mixed-nanoparticle groups. These are suggestive of nanoparticle-induced perturbation of glomerular filtration and tubule integrity, already reported in metal nanoparticle nephrotoxicity studies [62]. Histology of testes (Figure 12) was such that control animals had normal seminiferous tubule structure and organization of spermatogenic cells, but the groups given nanoparticles showed germ cell depletion, Sertoli cell vacuolation, interstitial edema, deformed basal lamina outlines, and necrobiotic changes disrupting spermatogenesis. These degradative inclinations are consistent with emerging evidence that AgNPs induce reproductive tissue structural damage by oxidative stress, mitochondrial damage, and integrity loss of the blood–testis barrier [83].

3.10. Relevance and translational limitations of the clinical and selected doses

Species dose translation is complex due to differences in metabolic rate, body surface area, and nanoparticle biodistribution. While conventional interspecies scaling models (e.g., body surface area scaling) might yield approximate values of human-equivalent doses **[84]**, these are far from being representative of the unique pharmacokinetic and toxicokinetic characteristics of nanoparticles, including agglomeration tendency, organ-specific deposition, and pathways of clearance. The doses, hence, for use in experiments need to be deemed exploratory but not clinically predictive. Moreover, comparison to clinically approved antimicrobial doses and toxicological reference points was not made in this study, which limits conclusions regarding human safety margins. Future studies need to include standardized methods of dose conversion, physiologically based pharmacokinetic (PBPK) modeling, and direct comparison to approved drug dosing in order to enhance the translational relevance of nanoparticle studies.

A limitation of one of the primary aspects of this work is the fact that a direct comparison was not made of the synthesized silver nanoparticles' (AgNPs) biological activity and safety profile with their counterparts of clinically approved antimicrobial agents or standardized toxicological references. Although our in vivo studies are revealing as to the potential efficacy and safety of green- and chemically synthesized AgNPs, the doses investigated were not directly comparable with those of human therapeutic exposure conditions. As a result, the clinical translation of the results is still restricted. Future studies must involve reference drugs, standardized toxicological endpoints, and dose-conversion procedures for improved evaluation of the clinical potential as well as the safety margins of the nanoparticles.

Conclusion

The main objective of this study was the formulation of AgNPs using the green approach, which has bio-friendly features as a hepatic-renal protection agent and may be safer and more biocompatible than synthetic medications. Pomegranate peel extract, which is rich in bioactive compounds, was utilized as a capping agent to stabilize the NPs after it was exploited as a reducing agent to produce nanoparticles. The biosynthesized AgNPs were characterized using UV-VIS, DLS, TEM and FTIR. Smaller-sized nanoparticles show better antioxidant activity. These results suggested that biosynthesized AgNPs have the ability to selectively repair the cellular morphology of the kidneys, liver and testes. However, more investigation is required to validate these results. Additional in vivo pharmaceutical investigation is required to clarify the manner in which AgNPs perform their mode of action by focusing on different genes. Likewise, different medications might be functionalized with these AgNPs to enable prolonged release of the drug at the body's site of action. Also, the mechanisms behind AgNPs' impacts on apoptosis require further investigation in order to create safe and efficient approaches to using them in a variety of applications.

Conflict of Interest

All authors declare no conflicts of interest.

Funding

No fund was received for this work.

References

[1] El-Baz, Y. G., Moustafa, A., Ali, M. A., El-Desoky, G. E., Wabaidur, S. M., & Faisal, M. M. (2023a). An Analysis of the Toxicity, Antioxidant, and Anti-Cancer Activity of Cinnamon Silver Nanoparticles in Comparison with Extracts and Fractions of *Cinnamomum Cassia* at Normal and Cancer Cell Levels. Nanomaterials, 13(5), 945. https://doi.org/10.3390/nano13050945

[2] Abo-El-Yazid, Z. H., Ahmed, O. K., El-Tholoth, M., & Ali, M. A. (2022). Green synthesized silver nanoparticles using *Cyperus rotundus* L. extract as a potential antiviral agent against infectious laryngotracheitis and infectious bronchitis viruses in chickens. Chemical and Biological Technologies in Agriculture, 9(1), 1-11. https://doi.org/10.1186/s40538-022-00325-z

[3] Zou, L.; Zhu, F.; Long, Z.E.; Huang, Y. (2021). Bacterial Extracellular Electron Transfer: A Powerful Route to the Green Biosynthesis of Inorganic Nanomaterials for Multifunctional Applications. J. Nanobiotechnol. 19, 120. https://doi.org/10.1186/s12951-021-00868-7

[4] El-Baz, Y. G., Moustafa, A., Ali, M. A., El-Desoky, G. E., Wabaidur, S. M., & Iqbal, A. (2023b). Green synthesized silver nanoparticles for the treatment of diabetes and the related complications of hyperlipidemia and oxidative stress in diabetic rats. Experimental Biology and Medicine, 248(23), 2237-2248. https://doi.org/10.1177/15353702231214258

[5] Luque-Jacobo, C.M.; Cespedes-Loayza, A.L.; Echegaray-Ugarte, T.S.; Cruz-Loayza, J.L.; Cruz, I.; de Carvalho, J.C.; Goyzueta- Mamani, L.D. (2023). Biogenic Synthesis of Copper Nanoparticles: A Systematic Review of Their Features and Main Applications. Molecules, 28, 4838. https://doi.org/10.3390/molecules28124838

[6] Ahmed, M., Marrez, D. A., Abdelmoeen, N. M., Mahmoud, E. A., Ali M. A., Decsi, K., & Tóth, Z. (2023a). Proximate analysis of Moringa oleifera leaves and the antimicrobial activities of successive leaf ethanolic and aqueous extracts compared with green chemically synthesized Ag-NPs and crude aqueous extract against some pathogens. *International Journal of Molecular Sciences*, *24*(4), 3529. https://doi.org/10.3390/ijms24043529

[7] Cameron S., Hosseinian F., Willmore W. (2018). A current Overview of the biological and cellular effects of nanosilver, Int. J. Mol. Sci. 19:2030. https://doi.org/10.3390/ijms24043529

[8] Iravani S., Korbekandi H., Mirmohammadi S.V., Zolfaghari B. (2014). Synthesis of silver nanoparticles: chemical, physical and biological methods, Res. Pharm. Sci. 9 (6) 385–406. https://pmc.ncbi.nlm.nih.gov/articles/PMC4326978/

[9] Ferdous, Z. and Nemmar, A. (2020). Health impact of silver nanoparticles: a review of the biodistribution and toxicity following various routes of exposure. International journal of molecular sciences, 21(7), 2375. https://doi.org/10.3390/ijms21072375

[10] Ahmed, M., Marrez, D. A., Abdelmoeen, N. M., Mahmoud, E. A., Ali, M. A. S., Decsi, K., & Tóth, Z. (2023b). Studying the Antioxidant and the Antimicrobial Activities of Leaf Successive Extracts Compared to the Green-Chemically Synthesized Silver Nanoparticles and the Crude Aqueous Extract from *Azadirachta indica*. Processes, 11(6), 1644. https://doi.org/10.3390/pr11061644

[11] Singh B., Singh J.P., Kaur A., Singh N. (2018). Phenolic compounds as beneficial phytochemicals in pomegranate (*Punica granatum* L.) peel: A review, Food Chem. 261:75–86. DOI: 10.1016/j.foodchem.2018.04.039

[12] Saparbekova A.A., Kantureyeva G.O., Kudasova D.E., Konarbayeva Z.K., Latif A.S. (2023). Potential of phenolic compounds from pomegranate (Punica granatum L.) byproduct with significant antioxidant and therapeutic effects: A narrative review", Saudi J. Biol. Sci. 30 (2):103553. https://doi.org/10.1016/j.sjbs.2022.103553

[13] Govindappa, M., Tejashree, S., Thanuja, V., Hemashekhar, B., Srinivas, C., Nasif, O. and Raghavendra, V. B. (2021). Pomegranate fruit fleshy pericarp mediated silver nanoparticles possessing antimicrobial, antibiofilm formation, antioxidant, biocompatibility and anticancer activity. Journal of Drug Delivery Science and Technology, 61, 102289. https://doi.org/10.1016/j.jddst.2020.102289

[14] Saad P.G., Castelino R.D., Ravi V., Al-Amri I.S., Khan S.A. (2021). Green synthesis of silver nanoparticles using Omani pomegranate peel extract and two polyphenolic natural products: characterization and comparison of their antioxidant, antibacterial, and cytotoxic activities, Beni-Suef Univ. J. Basic Appl. Sci. 10:1–10. asic and Applied Sciences (2021) https://doi.org/10.1186/s43088-021-00119-6

[15] Monika, P., Chandraprabha, M. N., Hari Krishna, R., Vittal, M., Likhitha, C., Pooja, N. and Chaudhary, V. (2022). Recent advances in pomegranate peel extract mediated nanoparticles for clinical and biomedical applications. Biotechnology and Genetic Engineering Reviews, 1-29. https://doi.org/10.1080/02648725.2022.2122299

[16] Creighton J.A., Blatchford C.G. and Albrecht M.G. (1979). Plasma resonance enhancement of Raman scattering by pyridine adsorbed on silver or gold sol particles of size comparable to the excitation wavelength. J Chem Soc Faraday Trans II, 75:790-8. DOI: 10.1039/F29797500790

[17] Suh JS, DiLella DP, Moskovits M. (1983). Surface-enhanced Raman spectroscopy of colloidal metal systems: a twodimensional phase equilibrium in p-aminobenzoic acid adsorbed on silver. J Phys Chem, 87:1540-4. https://doi.org/10.1021/j100232a018

[18] Sanganna, B.; Chitme, H.R.; Vrunda, K.; Jamadar, M.J. (2016). Antiproliferative and antioxidant activity of leaves extracts of Moringa oleifera. Int. J. Curr. Pharm. Rev. Res., 8:54–56. http://dx.doi.org/10.22159/ijcpr.2016v8i4.15278

[19] Fujimoto (1999). The Evolution of a Manufacturing System at Toyota. Oxford university press. ISBN: 0195352637, 9780195352634

[20] El-Moghazy M, El-Desoky M, El-Deeb M. (2014). Nutrational effect of linseed oil on productive performance, carcass characrtistic and blood picture of growing rabbits. Egyptian Journal of Rabbit Science, 28 (2): 287 -310. DOI: 10.21608/ejrs.2018.44116

[21] Reitman, S. and Frankel, S. (1957). A colorimetric method for the determination of serum glutamic oxaloacetic and glutamic pyruvic transaminases. Anal. J. Clin. Pathol.,28(1):56-63. https://doi.org/10.1093/ajcp/28.1.56

[22] Belfield, A. and Goldberg, D. (1971). Colorimetric determination of alkaline phosphatase activity. Enzyme, 12:561-566. https://doi.org/10.1159/000459586

[23] Walter, M. and Gerarde, H. (1970). Ultramicromethod for the determination of conjugated and total bilirubin in serum or plasma. Microchem. J., 15:231-236. https://doi.org/10.1016/B978-0-12-395630-9.50142-0

[24] Fawcett, J. K. and Scott, J. E. (1960). A rapid and precise method for the determination of urea. J. Clin. Pathol.,13:156-159. DOI: 10.1136/jcp.13.2.156

[25] Houot, O. (1985). Interpretation of clinical laboratory tests. *Biomedical publications*, 250. Elsevier. (1), 29-37. https://doi.org/10.1136/jcp.13.2.156

[26] Barham, D. and Trinder, P. (1972). Enzymatic determination of uric acid. Analyst., 97:142-145.

[27] Gornnall, A. G.; Bardawill, C. J. and David, M. M. (1949). Determination of serum proteins by means of the biuret reaction. J. Biol. Chem.,177(2):751-766. https://doi.org/10.1093/jaoac/70.1.1

[28] Doumas, B. T; Waston, W. A. and Biggs, M. G. (1971). Albumin standard and measurement of serum albumin and bromo cresol green. Clin. Chem. Act.,31:87-96. https://doi.org/10.1016/0009-8981(71)90365-2

[29] Fossati, P. and Prencipe, L. (1982). Serum triglycerides determined colorimetrically with an enzyme that produces hydrogen peroxide. Clin. Chem., 28(10):2077-2080. https://doi.org/10.1093/clinchem/28.10.2077

[30] Allain, C. C., Poon, L. S., Chan, C. S., Richmond, W. F. P. C., & Fu, P. C. (1974). Enzymatic determination of total serum cholesterol. *Clinical chemistry*, *20*(4), 470-475. https://doi.org/10.1093/clinchem/20.4.470

[31] Grove, T. H. (1979). Effect of reagent pH on determination of high-density lipoprotein cholesterol by precipitation with sodium phosphotungstate-magnesium. *Clinical chemistry*, *25*(4), 560-564. https://doi.org/10.1093/clinchem/25.4.560

[32] Friedewald, W. T., Levy, R. I., & Fredrickson, D. S. (1972). Estimation of the concentration of low-density lipoprotein cholesterol in plasma, without use of the preparative ultracentrifuge. *Clinical chemistry*, *18*(6), 499-502. https://doi.org/10.1093/clinchem/18.6.499

[33] Carleton H. M. (1980). Carleton's Histological Technique. 5th ed. RAB Drury and EA Wallington. (Pp 520; illustrated; £24.) Oxford Medical Publications. https://doi.org/10.1179/his.2006.29.2.99

[34] Fisher, F. M. (1970). Tests of equality between sets of coefficients in two linear regressions: An expository note. *Econometrica: Journal of the Econometric Society*, 361-366. https://doi.org/10.2307/1913018

[35] Waller, R. A., & Duncan, D. B. (1969). A Bayes rule for the symmetric multiple comparisons problem. *Journal of the American Statistical Association*, *64*(328), 1484-1503. https://doi.org/10.1080/01621459.1969.10501073

[36] Mulvaney P. (1996). Surface Plasmon Spectroscopy of Nanosized Metal Particles. Langmuir.12:788- 800. https://doi.org/10.1021/la9502711

[37] Huq, M.A. (2020). Green Synthesis of Silver Nanoparticles Using Pseudoduganella Eburnea MAHUQ-39 and Their Antimicrobial Mechanisms Investigation against Drug Resistant Human Pathogens. Int. J. Mol. Sci., 21, 1510. DOI: 10.3390/ijms21041510

[38] Veerasamy, R.; Xin, T.Z.; Gunasagaran, S.; Xiang, T.F.W.; Yang, E.F.C.; Jeyakumar, N.; Dhanaraj, S.A. Biosynthesis of Silver Nanoparticles Using Mangosteen Leaf Extract and Evaluation of Their Antimicrobial Activities. J. Saudi Chem. Soc. 2011, 15, 113–120. https://doi.org/10.1016/j.jscs.2010.06.004

[39] Traiwatcharanon, P.; Timsorn, K.; Wongchoosuk, C. (2015). Effect of PH on the Green Synthesis of Silver Nanoparticles through Reduction with *Pistiastratiotes* L. Extract. Adv. Mater. Res., 1131, 223–226. https://doi.org/10.4028/www.scientific.net/AMR.1131.223

[40] GnanaJobitha G., Annadurai G. and Kannan C. (2012). Green synthesis of silver nanoparticle using Elettaria cardamomom and assessment of its antimicrobial activity. Int J Pharma Sci Res. 3:323-330. ISSN : 0975-9492

[41] Anith Jose, R.; Devina Merin, D.; Arulananth, T.S.; Shaik, N. (2022). Characterization Analysis of Silver Nanoparticles Synthesized from *Chaetoceros calcitrans*. J. Nanomater., 2022, 4056551. https://doi.org/10.1155/2022/4056551

[42] Hassan M.G., Farouk H.S., Baraka D.M., Khedr M., El Awady M.E., Ameen F., Sajjad Z., Elmetwalli A. (2024). Pomegranate's silver bullet: Nature-powered nanoparticles deliver a one-two punch against cancer and antimicrobial resistance. Inorganic Chemistry Communications 168 (2024) 112853. https://doi.org/10.1016/j.inoche.2024.112853

[43] Huong V.T.L., Nguyen N.T. (2021). Green synthesis, characterization and antibacterial activity of silver nanoparticles using *Sapindus mukorossi* fruit pericarp extract, Mater. Today Proc. 42:88–93. https://doi.org/10.1016/j.matpr.2020.10.015

[44] Galatage, S. T., Hebalkar, A. S., Dhobale, S. V., Mali, O. R., Kumbhar, P. S., Nikade, S. V., and Killedar, S. G. (2021). Silver nanoparticles: properties, synthesis, characterization, applications and future trends. Chapter 4. Silver micro-nanoparticles—Properties, synthesis, characterization, and applications. DOI: 10.5772/intechopen.99173

[45] Nangare S.N., Patil P.O. (2020). Green synthesis of silver nanoparticles: An eco-friendly approach, Nano Biomed. Eng. 12 (4) 281–296. DOI: 10.5101/nbe.v12i4.p281-296

[46] Vadakkan K., Rumjit N.P., Ngangbam A.K., Vijayanand S., Nedumpillil N.K. (2024). Novel advancements in the sustainable green synthesis approach of silver nanoparticles (AgNPs) for antibacterial therapeutic applications, Coord. Chem. Rev. 499; 215528. https://doi.org/10.1016/j.ccr.2023.215528

[47] Rónavári, A., Igaz, N., Adamecz, D. I., Szerencsés, B., Molnar, C., Kónya, Z., ... & Kiricsi, M. (2021). Green silver and gold nanoparticles: Biological synthesis approaches and potentials for biomedical applications. *Molecules*, *26*(4), 844. https://doi.org/10.3390/molecules26040844

[48] Aly A.A., Fahmy H.M. and Abou-Okeil A. (2024). Green synthesis of silver nanoparticles using commercially available starch products. Egypt. J. Chem. Vol. 67: (1); 309 – 317. https://doi.org/10.3390/molecules26040844

[49] Yaqoob A.A., Umar K., Ibrahim M.N.M. (2020). Silver nanoparticles: various methods of synthesis, size affecting factors and their potential applications–a review, Appl. Nanosci. 10; 1369–1378. Applied Nanoscience (2020) 10:1369–1378 https://doi.org/10.1007/s13204-020-01318-w

[50] Jadhav K., Dhamecha D., Bhattacharya D., Patil M. (2016). Green and ecofriendly synthesis of silver nanoparticles: Characterization, biocompatibility studies and gel formulation for treatment of infections in burns, J. Photochem. Photobiol. B Biol. 155; 109–115. https://doi.org/10.1016/j.jphotobiol.2016.01.002

[51] Nandiyanto A.B.D., Oktiani R., Ragadhita R. (2019). How to read and interpret FTIR spectroscope of organic material, Indones. J. Sci. Technol. 4:(1); 97–118. http://dx.doi.org/10.17509/ijost.v4i1.xxxx

[52] Farouk, S.M.; Abu-Hussien, S.H.; Abd-Elhalim, B.T.; Mohamed, R.M.; Arabe, N.M.; Hussain, A.A.T.; Mostafa, M.E.; Hemdan, B.; El-Sayed, S.M.; Bakry, A.; et al. (2023). Biosynthesis and Characterization of Silver Nanoparticles from Punica Granatum (Pomegranate) Peel Waste and Its Application to Inhibit Foodborne Pathogens. *Sci. Rep.*, *13*, 19469. https://doi.org/10.1038/s41598-023-46355-x

[53] Manimaran, K., Yanto, D. H. Y., Anita, S. H., Nurhayat, O. D., Selvaraj, K., Basavarajappa, S., and Kumarasamy, K. (2023). Synthesis and characterization of Hypsizygus ulmarius extract mediated silver nanoparticles (AgNPs) and test their potentiality on antimicrobial and anticancer effects. Environmental Research, 235, 116671. https://doi.org/10.1016/j.envres.2023.116671

[54] Widatalla, H. A., Yassin, L. F., Alrasheid, A. A., Ahmed, S. A. R., Widdatallah, M. O., Eltilib, S. H., and Mohamed, A. A. (2022). Green synthesis of silver nanoparticles using green tea leaf extract, characterization and evaluation of antimicrobial activity. Nanoscale Advances, 4(3), 911-915. https://doi.org/10.1039/D1NA00509J

[55] Alzubaidi, A. K., Al-Kaabi, W. J., Ali, A. A., Albukhaty, S., Al-Karagoly, H., Sulaiman, G. M., and Khane, Y. (2023). Green synthesis and characterization of silver nanoparticles using flaxseed extract and evaluation of their antibacterial and antioxidant activities. Appl. Sci., 13(4), 2182. https://doi.org/10.3390/app13042182

[56] Hanafy, E. A., Shanab, S. M., Hafez, R. M., & Shalaby, E. A. (2025). Using of Expired Silymarin Medication as A Source of Biologically Active Compounds and Green Synthesis of Nanoparticles. Egyptian Journal of Chemistry, 68(9), 365-375. 10.21608/ejchem.2025.346672.11028

[57] Goodarzi, V.; Zamani, H.; Bajuli, L. and Moradshahi, A. (2014). Evaluation of antioxidant potential and reduction capacity of some plant extracts in silver nanoparticles' synthesis. Mol. Biol. Res. Commun., 3, 165. https://pmc.ncbi.nlm.nih.gov/articles/PMC5019224/

[58] Ghaffari-Moghaddam, M.; Hadi-Dabanlou, R.; Khajeh, M.; Rakhshanipour, M.; Shameli, K. (2014). Green synthesis of silver nanoparticles using plant extracts. Korean J. Chem. Eng., 31, 548–557. DOI: 10.1007/s11814-014-0014-6

[59] Tyagi, P. K., Tyagi, S., Gola, D., Arya, A., Ayatollahi, S. A., Alshehri, M. M., and Sharifi-Rad, J. (2021). Ascorbic acid and polyphenols mediated green synthesis of silver nanoparticles from *Tagetes erecta* L. aqueous leaf extract and studied their antioxidant properties. J. Nanomater, 2021: (1); 6515419. https://doi.org/10.1155/2021/6515419

[60] Erenler R. and Dag B. (2022). Biosynthesis of silver nanoparticles using Origanum majorana L. and evaluation of their antioxidant activity. Inorg. Nano-Met. Chem., 52: (4); 485–492. https://doi.org/10.1080/24701556.2021.1952263

[61] Sarin, S. K., & Choudhury, A. (2018). Management of acute-on-chronic liver failure: an algorithmic approach. *Hepatology international*, *12*(5), 402-416. https://doi.org/10.1007/s12072-018-9887-5

[62] Johnston, H. J., Hutchison, G., Christensen, F. M., Peters, S., Hankin, S., & Stone, V. (2010). A review of the in vivo and in vitro toxicity of silver and gold particulates: particle attributes and biological mechanisms responsible for the observed toxicity. *Critical reviews in toxicology*, *40*(4), 328-346. https://doi.org/10.3109/10408440903453074

[63] Kim, Y. S., Song, M. Y., Park, J. D., Song, K. S., Ryu, H. R., Chung, Y. H., ... & Yu, I. J. (2010). Subchronic oral toxicity of silver nanoparticles. *Particle and fibre toxicology*, *7*(1), 20. https://doi.org/10.1186/1743-8977-7-20

[64] Kose, O., Mantecca, P., Costa, A., & Carrière, M. (2023). Putative adverse outcome pathways for silver nanoparticle toxicity on mammalian male reproductive system: a literature review. *Particle and Fibre Toxicology*, *20*(1), 1. https://doi.org/10.1186/s12989-022-00511-9

[65] Recordati, C., De Maglie, M., Bianchessi, S., Argentiere, S., Cella, C., Mattiello, S., ... & Scanziani, E. (2015). Tissue distribution and acute toxicity of silver after single intravenous administration in mice: nano-specific and size-dependent effects. *Particle and fibre toxicology*, *13*(1), 12. https://doi.org/10.1186/s12989-016-0124-x

[66] Braakhuis, H. M., Cassee, F. R., Fokkens, P. H., De La Fonteyne, L. J., Oomen, A. G., Krystek, P., ... & Park, M. V. (2016). Identification of the appropriate dose metric for pulmonary inflammation of silver nanoparticles in an inhalation toxicity study. *Nanotoxicology*, *10*(1), 63-73. https://doi.org/10.3109/17435390.2015.1012184

[67] Das, S. K., Sen, K., Ghosh, B., Ghosh, N., Sinha, K., & Sil, P. C. (2024). Molecular mechanism of nanomaterials induced liver injury: A review. *World Journal of Hepatology*, *16*(4), 566. doi: 10.4254/wjh.v16.i4.566

[68] Culling CF, Allison RT, Barr WT. (1985). Cellular Pathology Technique. 4 th ed. New York: Butterworth, 642 p. Doi: 10.1016/C2013-0- 06260-3.

[69] Park E, Bae Y, Kim Y, Choi K, Lee SH. (2010). Reapted - dose toxicity and inflammatory responses in mice by oral administration of silver nanoparticles.30:162-168. Doi: 10.1016/j.etap.2010.05.004.

[70] Hauck TS, Anderson RE, Fischer HC, Newbigging S, Chan WC. (2010). *In vivo* quantum-dot toxicity assessment. 6(1):138-144. Doi: 10.1002/smll.200900626 https://doi.org/10.1002/smll.200900626

[71] Rajendoran V, Krishnaswamy K. (2016). Effect of Solanum villosum extract and its silver nanoparticles on hematopoietic system of diethylnitrosamine-induced hepatocellular carcinoma in rats. Inno J of Health Sci. 5(1):13-16. ID:212550217.

[72] Morones JR, Elechinguerra JL, Camacho A, Holt K, Kouri JB, Ramirez JT, Yacaman MJ. (2005). The bacterial effect of silver nanoparticles. Nanotechnol. 16(10):2346-53. DOI 10.1088/0957-4484/16/10/059

[73] Nirmala R, Sheikh FA, Kanjwal MA, Lee JH, Park S, Navamthavan R, Kim HY. Synthesis and characterization of bovine femurbone hydroxyapatite containing silver nanoparticles for the biomedical applications. J Nano Res. 2011; 13:1917-1927. Doi: 10. 1007/ s11051- 010-9944-z

[74] Mocan T, Clichici S, Agoston CL, Simon S, Ilie, IR, Biris AR, Muresan A. (2010). Implication of oxidative stress mechanisms in toxicity of nanoparticles (review). Acta Physiol Hung. 97(3):247-255. https://doi.org/10.1556/aphysiol.97.2010.3.1

[75] Al-Baker, A. A., Al-Kshab, A. A., Ismail, H. K., and Ashwaq, A. H. (2020). Effect of silver nanoparticles on some blood parameters in rats. Iraqi J Vet Sci, 34(2), 389-395. DOI: 10.33899/ijvs.2019.126116.1243.

[76] Jeong G.N., Jo U.B., Ryu H.Y., Kim Y.S., Song K.S. and Yu I.J. (2010). Histochemical study of intestinal mucins after administration of silver nanoparticles in Sprague Dawley rats. Arch Toxicol, 84(1):63-9. DOI 10.1007/s00204-009-0469-0

[77] Zhang, R.; Qin, X.; Zhang, T.; Li, Q.; Zhang, J.; Zhao, J. (2018). Astragalus polysaccharide improves insulin sensitivity via AMPK activation in 3T3-L1 adipocytes. Molecules 2018, 23, 2711. https://doi.org/10.3390/molecules23102711

[78] Alkaladi, A.; Abdelazim, A.M.; Afifi, M. (2014). Antidiabetic activity of zinc oxide and silver nanoparticles on streptozotocin-induced diabetic rats. Int. J. Mol. Sci., 15, 2015–2023. https://doi.org/10.3390/ijms15022015

[79] Mousavi B, Tafvizi F, Zaker Bostanabad S. (2018). Green synthesis of silver nanoparticles using Artemisia turcomanica leaf extract and the study of anti-cancer effect and apoptosis induction on gastric cancer cell line (AGS). Artif Cells Nanomed https://doi.org/10.1080/21691401.2018.1430697

[80] Aslany S., Tafvizi F. and Naseh V. (2020). Characterization and evaluation of cytotoxic and apoptotic effects of green synthesis of silver nanoparticles using Artemisia Ciniformis on human gastric adenocarcinoma. Mater Today Commun; 24:101011. https://doi.org/10.1016/j.mtcomm.2020.101011

[81] Edlich F. (2018). BCL-2 proteins and apoptosis: recent insights and unknowns. Biochem Biophys Res Commun; 500:26-34.

[82] Soni D. and Gandhi D. (2024). Toxicity evaluation of silver nanoparticles synthesized from naringin flavonoid on human promyelocytic leukemic cells and human blood cells. Toxicol. Indust. Health, 40: (3); 125–133. https://doi.org/10.2174/0118761429273223231124072223

[83] Rana, S. V. S. (2021). Recent advances on renal toxicity of engineered nanoparticles—a review. J. Toxicol. Risk Assess, *7*, 36. https://doi.org/10.23937/2572-4061.1510036

[84] Reagan-Shaw, S., Nihal, M., & Ahmad, N. (2008). Dose translation from animal to human studies revisited. The FASEB journal, 22(3), 659-661. https://doi.org/10.1096/fj.07-9574LSF